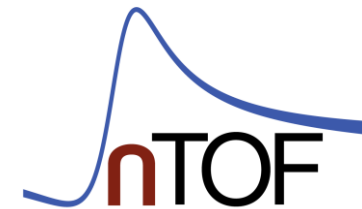


# $^{50}\text{Cr}$ and $^{53}\text{Cr}$ (n, $\gamma$ ) cross section measurements at n\_TOF and HiSPANoS

P. PÉREZ-MAROTO, C. GUERRERO, A. CASANOVAS,  
B. FERNÁNDEZ & THE N\_TOF COLLABORATION.

---

WONDER 2026, AIX-EN-PROVENCE. 30/06/2026



# Index

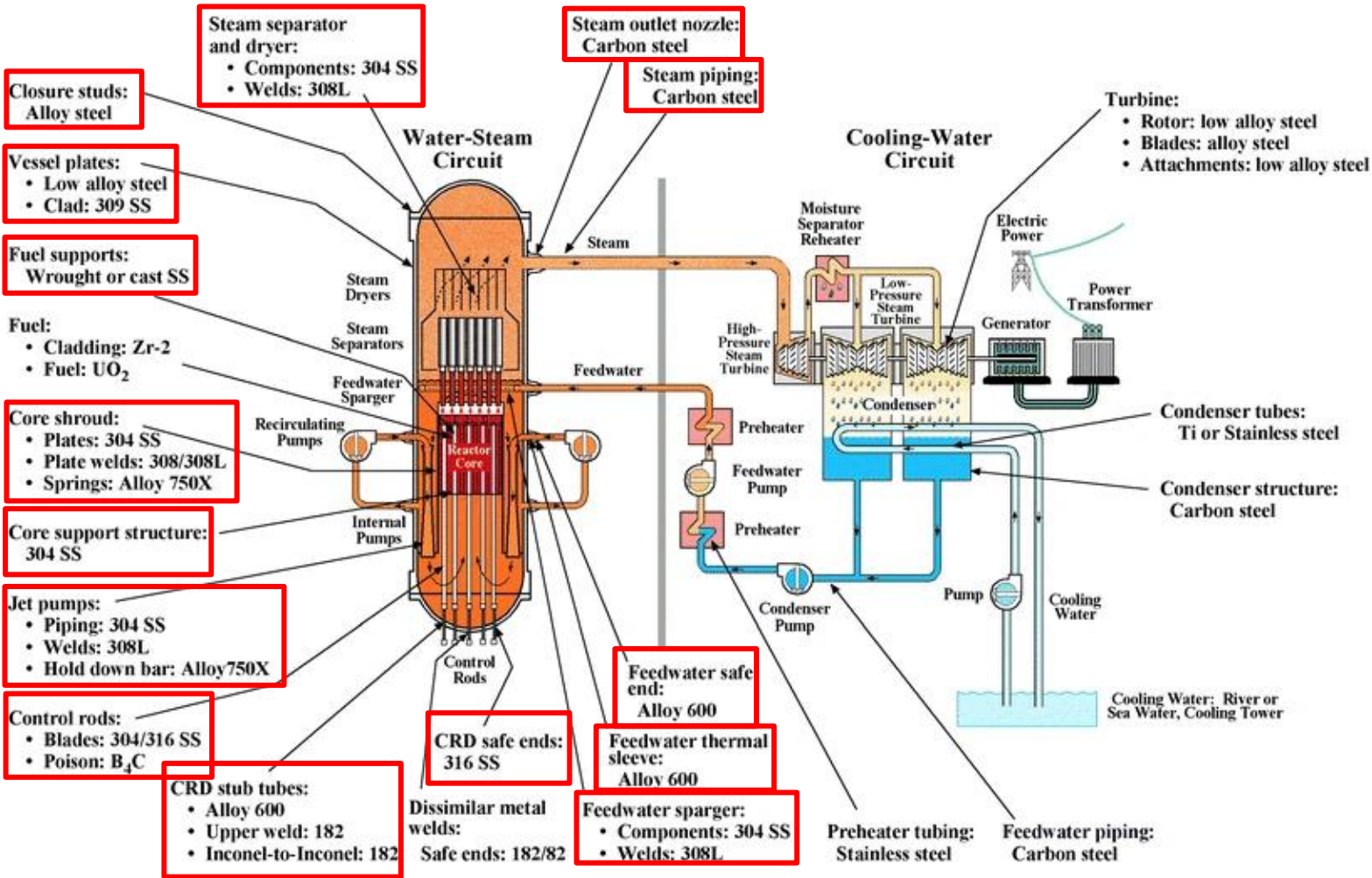
- I. Introduction
- II.  $^{50}\text{Cr}$  activation measurement at HiSPANoS
- III.  $^{50,53}\text{Cr}$  time-of-flight measurement at EAR1-n\_TOF
- IV. Summary & Conclusions



P. Pérez-Maroto PhD: *“Measurement of  $^{50}\text{Cr}$  and  $^{53}\text{Cr}$  neutron capture cross sections for nuclear technology at CERN n\_TOF and HiSPANoS”*

# I. Introduction

# Why $^{50,53}\text{Cr}$ neutron capture?



- **Stainless Steel** → structural material in nuclear reactors.
- Contains 11-26% of chromium.
- Criticality benchmarks sensitive to chromium → dominated by  $^{50,53}\text{Cr} (n, \gamma)$
- ~30% discrepancies in  $^{50}\text{Cr}$  and  $^{53}\text{Cr}$  cross sections → 1% change in  $k_{\text{eff}}^\dagger$ .


<sup>†</sup>A. Trkov, “On the Benchmarking of New Evaluated Nuclear Data Libraries”, INDC (NDS)-0751 (2018)

# Why $^{50,53}\text{Cr}$ neutron capture?

## NEA Nuclear Data High Priority Request List, HPRL

HPRL Main	High Priority Requests (HPR)	General Requests (GR)	Special Purpose Quantities (SPQ)		New Request	EG-HPRL (SG-C)
			Standard	Dosimetry		

Request ID	98		Type of the request	High Priority request		
Target	Reaction and process	Incident Energy	Secondary energy or angle	Target uncertainty	Covariance	
24-CR-53	(n,g) SIG	1 keV-100 keV		8-10	Y	
Field	Subfield	Created date	Accepted date	Ongoing action	Archived Date	
Fission		20-JAN-18	05-FEB-18	Y		

 Send a comment on this request to NEA.

**Requester:** Dr Roberto CAPOTE NOY at IAEA, AUT

**Email:** roberto.capotenoy@iaea.org

**Project (context):**

**Impact:**

Neutron absorption in the Cr isotopes of structural materials affects the criticality of fast reactor assemblies [Koscheev2017]. These cross sections are also of interest for stellar nucleosynthesis [Kadonis10].

**Accuracy:**

8-10% in average cross-sections and calculated MACS at 10, 30, 100 keV.

Selected criticality benchmarks with large amounts of Cr (e.g., PU-MET-INTER-002, and HEU-COMP-INTER-005/4=KBR-15/Cr) show large criticality changes of the order of 1000 pcm due to 30% change in Cr-53 capture in the region from 1 keV up to 100 keV [Trkov2018]. On the other side different evaluations (e.g., BROND-3.1, ENDF/B-VII.1, ENDF/B-VIII.0 and JEFF-3.3) for Cr-53(n,g) are discrepant by 30% in the same energy region. For Cr-50, evaluated files show better agreement at those energies but they are lower than Mughabghab evaluation of the resonance integral by 35%. These discrepancies are not reflected in estimated uncertainty of the evaluated files (e.g., JEFF-3.3 uncertainty is around 10% which is inconsistent with the observed spread in evaluations). Due to these differences we request new capture data with 8-10% uncertainty to discriminate between different evaluations and improve the C/E for benchmarks containing Chromium and/or SS.

**Justification document:**

Criticality benchmarks can test different components of stainless steel (SS), including Cr which is a large component of some SS. Currently, a large part of the uncertainty in SS capture seems to be driven by uncertainty in Cr capture [Koscheev2017]. Indeed, some benchmarks highly sensitive to Cr (as a component of SS) indicate a need for much higher capture in Cr for both Pu and U fueled critical assemblies (e.g., HEU-COMP-INTER-005/4=KBR-15/Cr and PU-MET-INTER-002=ZPR-6/10).

- **Stainless Steel** → structural material in nuclear reactors.
- Contains 11-26% of chromium.
- Criticality benchmarks sensitive to chromium → dominated by



- ~30% discrepancies in  $^{50}\text{Cr}$  and  $^{53}\text{Cr}$  cross sections → 1% change in  $k_{\text{eff}}^{\dagger}$ .



**NEA High Priority Request List (HPRL):**  
 **$^{50,53}\text{Cr} \sigma(n, \gamma)$  within 8-10% from 1 to 100 keV**

<sup>†</sup>A. Trkov, “On the Benchmarking of New Evaluated Nuclear Data Libraries”, INDC (NDS)-0751 (2018)

# Previous measurements and evaluations

Several measurements have been performed during the 70s and 80s, and a more recent one in ORELA by Guber et al. (2011) <sup>†</sup>.

Experiment	Stieglitz (1971)	Beer (1975)	Kenny (1977)	Brusegan (1986)	Guber (2011)
Facility	RPI	FZK	ORELA	GELINA	ORELA
Detector	Scin.tank	Scin.tank	C <sub>6</sub> F <sub>6</sub>	C <sub>6</sub> D <sub>6</sub>	C <sub>6</sub> D <sub>6</sub>
<u>Thickness <sup>50</sup>Cr (10<sup>-3</sup> at/barns)</u>	8	18	5/8	7	-
<u>Thickness <sup>53</sup>Cr (10<sup>-3</sup> at/barns)</u>	14	14	8/12	12/60	14

- Goal: as many resonances as possible, even at high energies.
- Very **thick samples** were used → large **neutron multiple-scattering** effects.

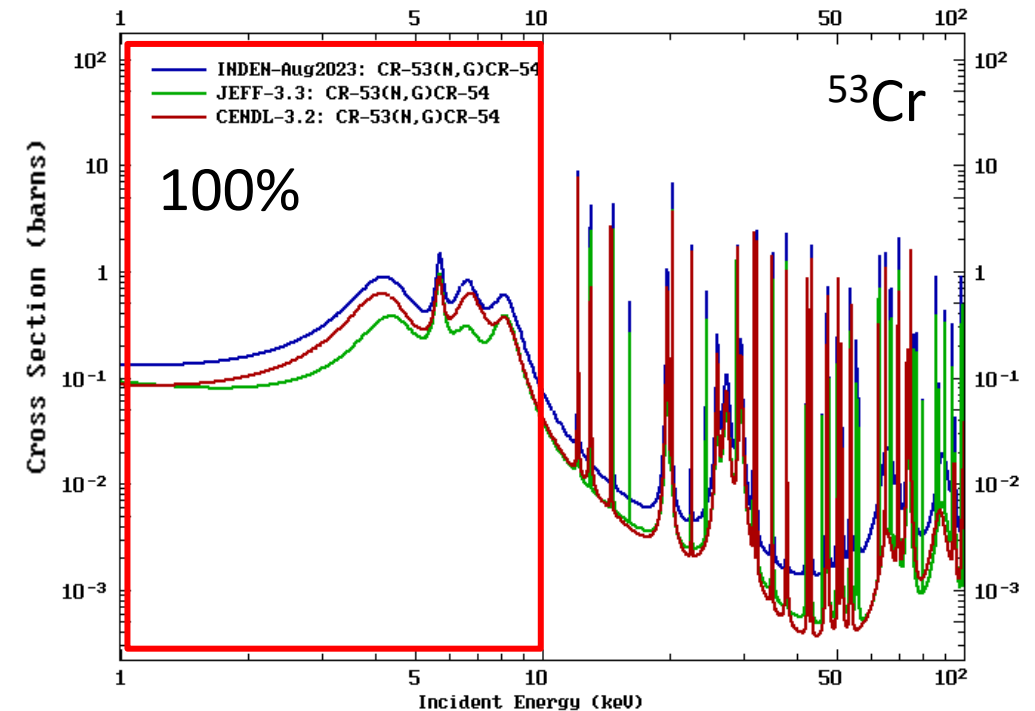
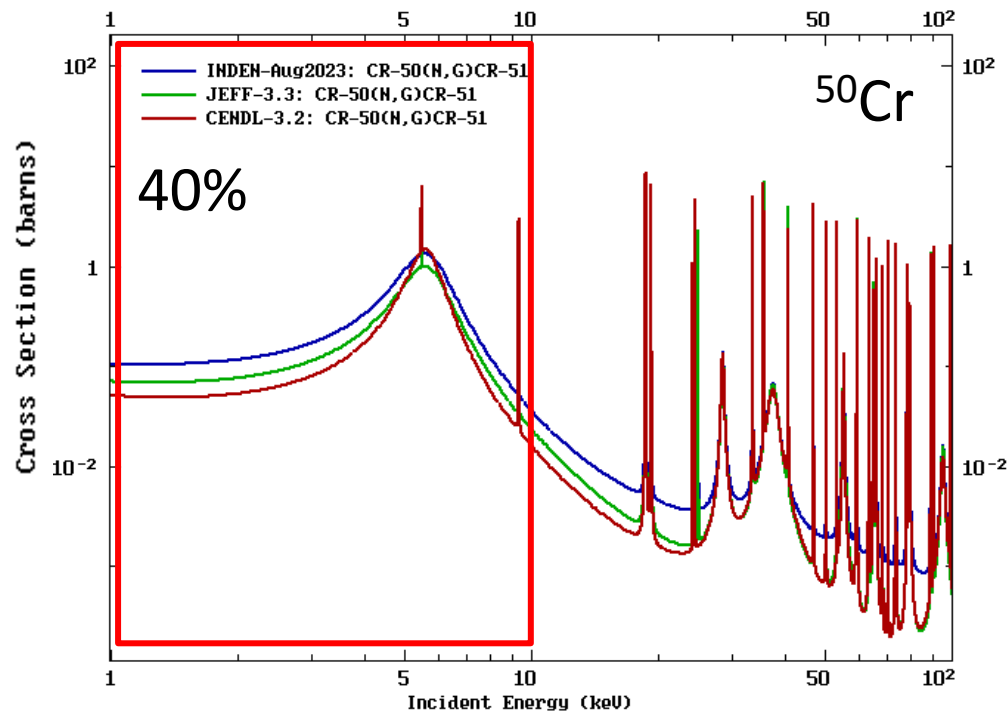
Guber improves the neutron sensitivity → Issues with sample characterization.

<sup>†</sup>K. H. Guber et al., “Neutron cross-section measurements on structural materials at ORELA”, J. Korean Phys. 59, n° 2(3) (2011)

# Previous measurements and evaluations

## Evaluated data

- JEFF-3.3, ENDF/B-VIII.0 & JENDL-5 → Same XS, mainly based on Guber et al (2011).
- CENDL-3.2 → Uses data from the 70's and 80's.
- INDEN → Careful re-evaluation of multiple-scattering effects at Guber et al. data.
- ENDF/B-VIII.1, JEFF-4.0 → Has adopted INDEN.



## II. $^{50}\text{Cr}$ activation measurement at HiSPANoS@CNA

# The HiSPANoS facility at CNA



# HiSPANoS

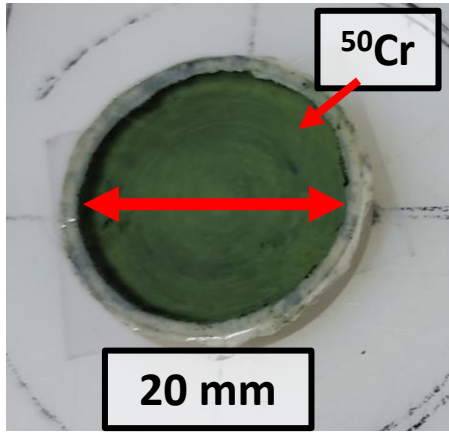
HiSPANoS is the neutron facility of CNA †‡.

- Thermal (eV) → moderation
- Epithermal (keV) → Li(p,n)
- Fast (MeV) →  ${}^2\text{H}(d,n)$  and Be/Li(p/d,n)
  - Continuous: activations/irradiations
  - Pulsed: ToF measurements

†M. Macías et al., “*The first neutron time-of-flight line in Spain: ...*”, Rad. Phys. and Chem. 168 (2020)

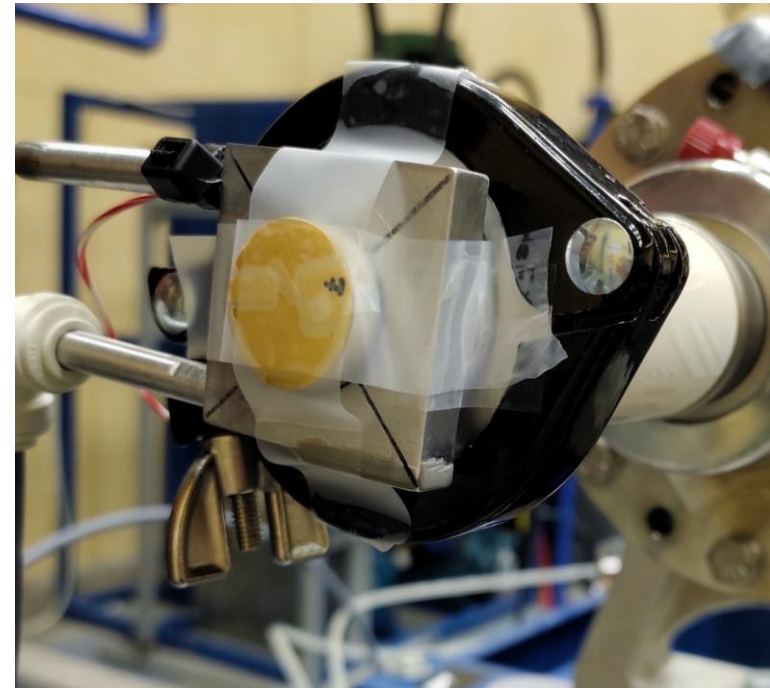
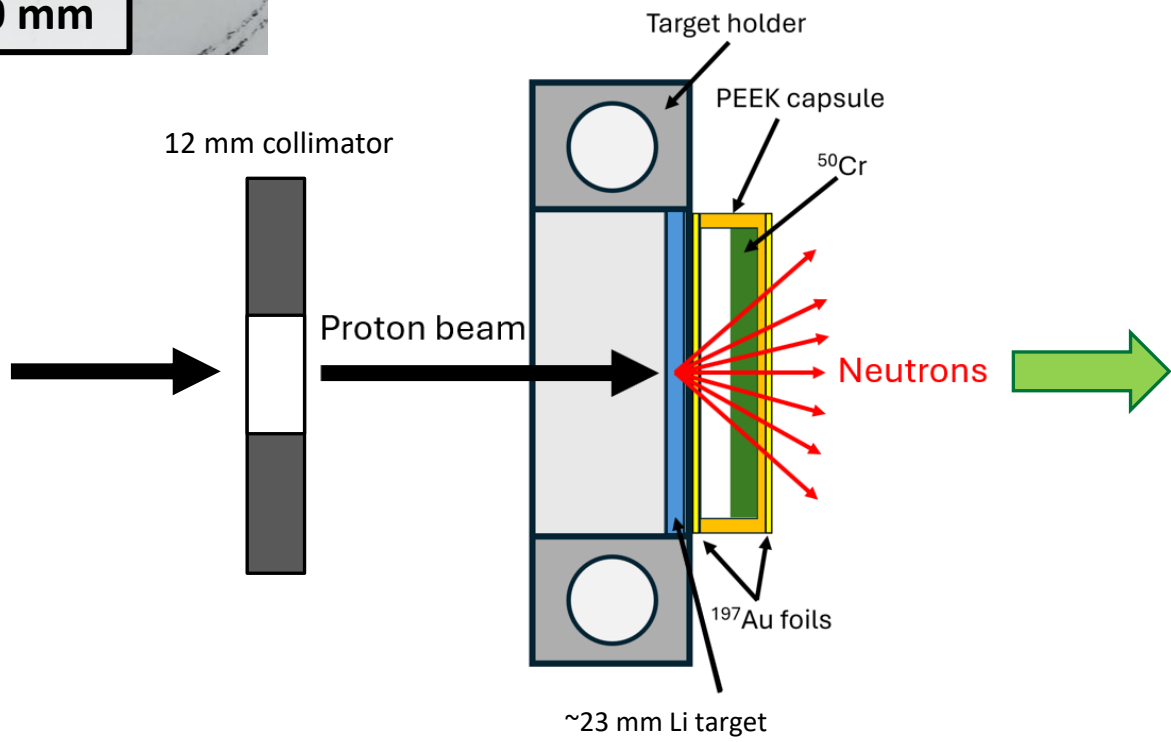
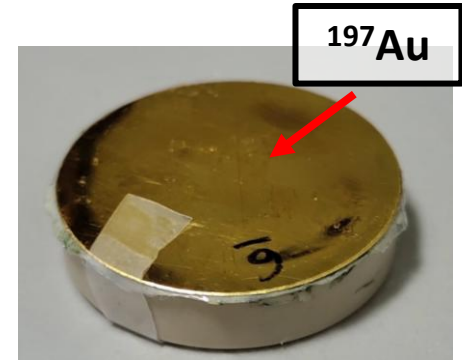
‡M. A. Millán-Callado et al., “*Continuous and pulsed fast neutron beams at the CNA HiSPANoS facility*”, Rad. Phys. and Chem. 217 (2024)

# Experimental set-up. Activation sample

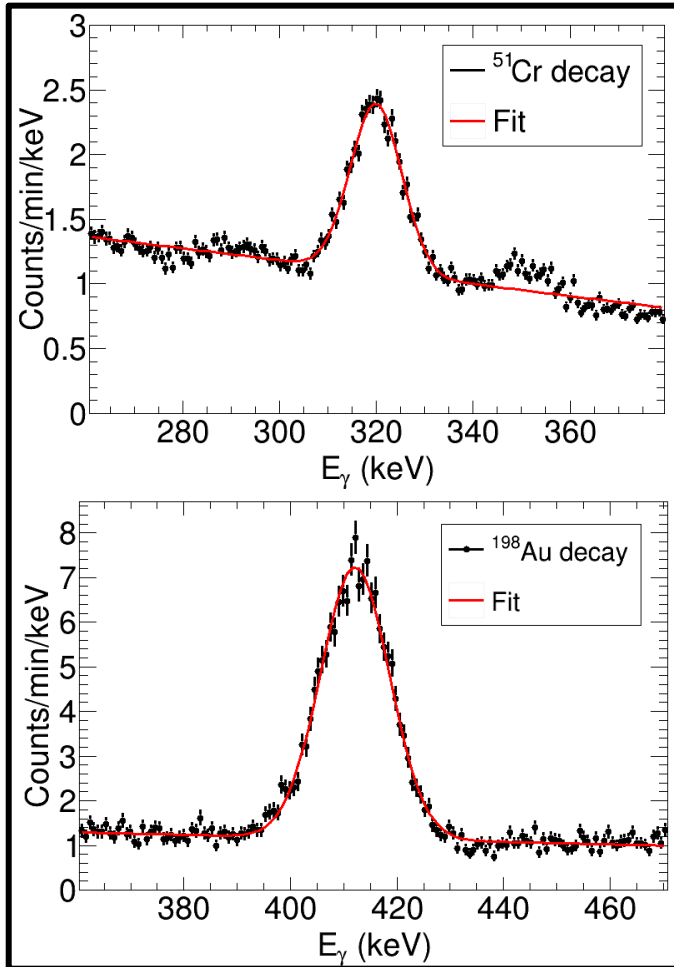


- 94.6(4)% enriched  $^{50}\text{Cr}_2\text{O}_3$
- 723(3) mg of material
- Inside a PEEK capsule

Measured relative to two  $^{197}\text{Au}$  foils (standard cross section)



# Neutron activation analysis



$$N_{act} = \frac{A_{EOI}}{\lambda} = \frac{C \cdot e^{\lambda t_{wait}} \cdot f_{irr}}{I_{\gamma} \cdot \varepsilon \cdot (1 - e^{-\lambda t_{meas}})}$$

	$N_{act}(10^6)$
$^{50}\text{Cr}$	79(3)
$^{197}\text{Au}_{\text{front}}$	434(11)
$^{197}\text{Au}_{\text{back}}$	425(10)

Efficiency is the main source of uncertainty

	$^{50}\text{Cr}$ (%)	$^{197}\text{Au}_{\text{front}}$ (%)	$^{197}\text{Au}_{\text{back}}$ (%)
$I_{\gamma}$	0.1	0.6	
$\varepsilon$	3.3	1.8	
$C$	1.3	1.7	1.5
$e^{\lambda t_w}$	0.01	0.08	0.07
$e^{-\lambda t_m}$	0.01	0.01	
$f_{irr}$	0.2	0.2	
<b>Overall</b>	<b>3.6</b>	<b>2.6</b>	<b>2.4</b>

# MACS<sub>30</sub>(<sup>50</sup>Cr) determination

$$\langle \sigma \rangle = \frac{\int \sigma_{\gamma}(E_n) \Phi(E_n) dE_n}{\int \Phi(E_n) dE_n} \rightarrow$$

If  $\Phi$  is a Maxwellian distribution  
at a temperature of  $kT$  (keV)



$$\text{MACS}_{kT} = \frac{2}{\sqrt{\pi}} \langle \sigma \rangle_{kT}$$

# MACS<sub>30</sub>(<sup>50</sup>Cr) determination

$$\langle \sigma \rangle = \frac{\int \sigma_{\gamma}(E_n) \Phi(E_n) dE_n}{\int \Phi(E_n) dE_n} \rightarrow$$

If  $\Phi$  is a Maxwellian distribution at a temperature of kT (keV)



$$\text{MACS}_{kT} = \frac{2}{\sqrt{\pi}} \langle \sigma \rangle_{kT}$$

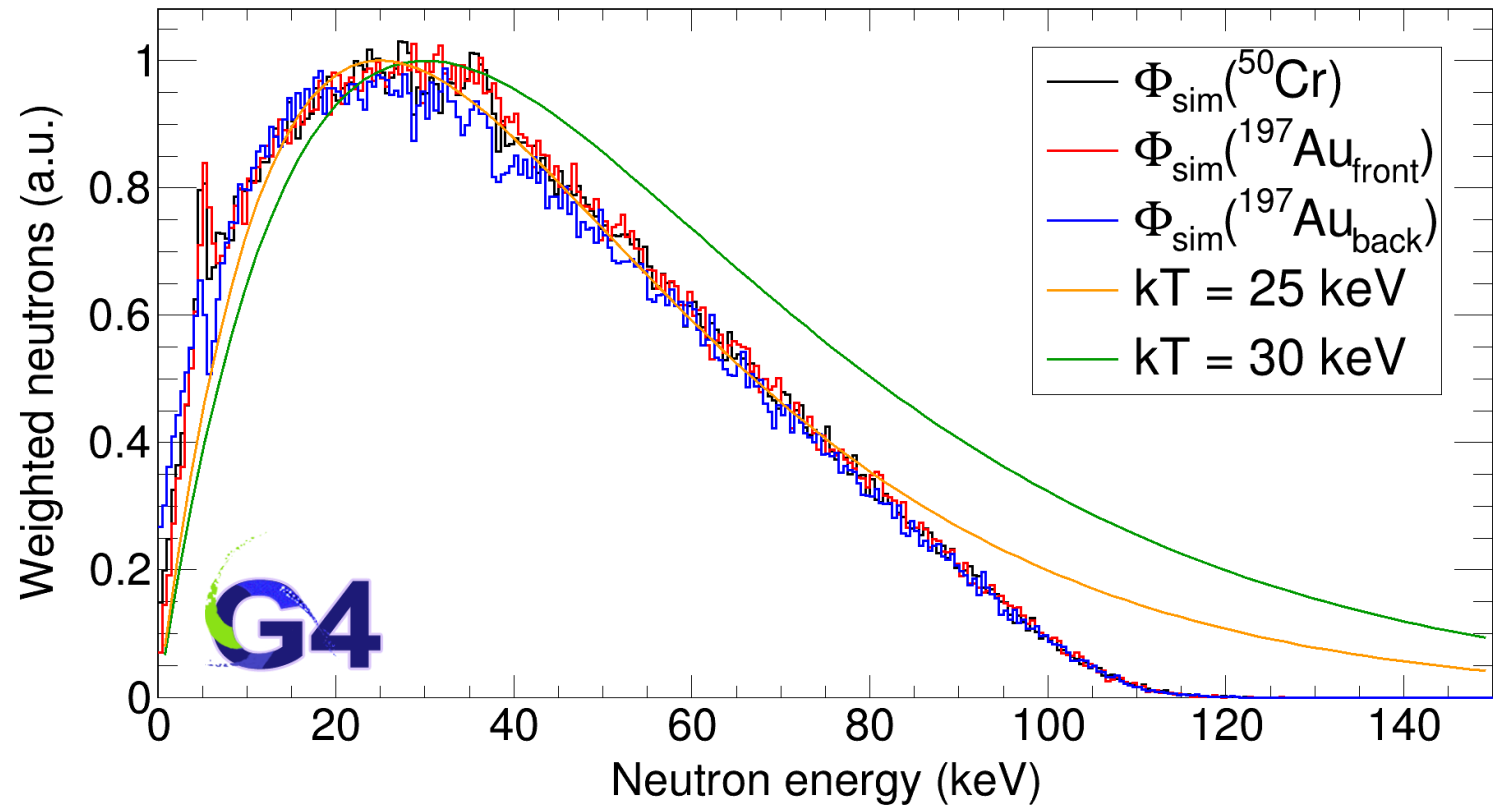
MACS<sub>30</sub>(<sup>50</sup>Cr) relative to MACS<sub>30</sub>(<sup>197</sup>Au):

$$\frac{\langle \sigma \rangle_{sim,Cr}}{\langle \sigma \rangle_{sim,Au}} = \frac{N_{act,Cr}}{n_{at,Cr}} \frac{n_{at,Au}}{N_{act,Au}} f_{\Phi}$$



SimLiT + GEANT4

$$\text{MACS}_{30}(\text{}^{50}\text{Cr}) = \frac{2}{\sqrt{\pi}} f_{S \rightarrow M} \langle \sigma \rangle_{sim, \text{}^{50}\text{Cr}}$$

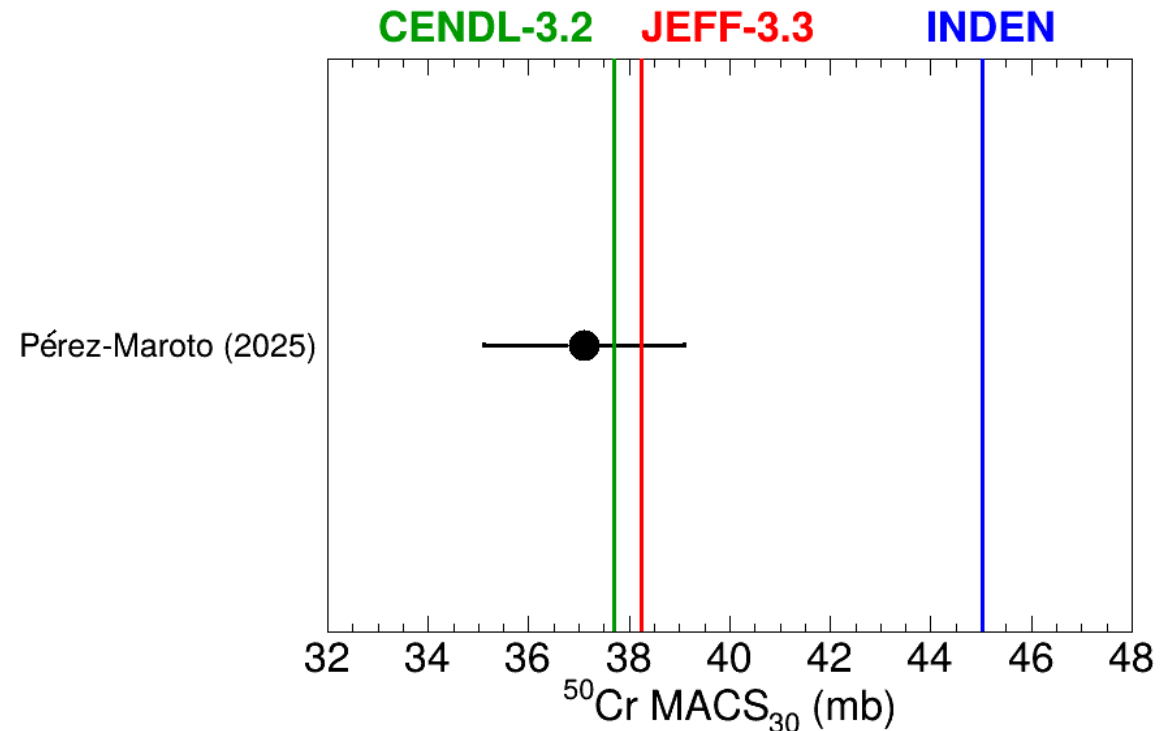


# MACS<sub>30</sub>(<sup>50</sup>Cr). Comparison with previous data

- First <sup>50</sup>Cr neutron activation measurement.
- Agreement with CENDL-3.2 and JEFF-3.3 (and therefore, ENDF/B-VIII.0 and JENDL-5).
- 20% lower than INDEN.

MACS <sub>30</sub> ( <sup>50</sup> Cr)	<sup>197</sup> Au <sub>front</sub>	<sup>197</sup> Au <sub>back</sub>
JEFF-3.3	37.9 mb	38.5 mb
INDEN	35.7 mb	36.4 mb

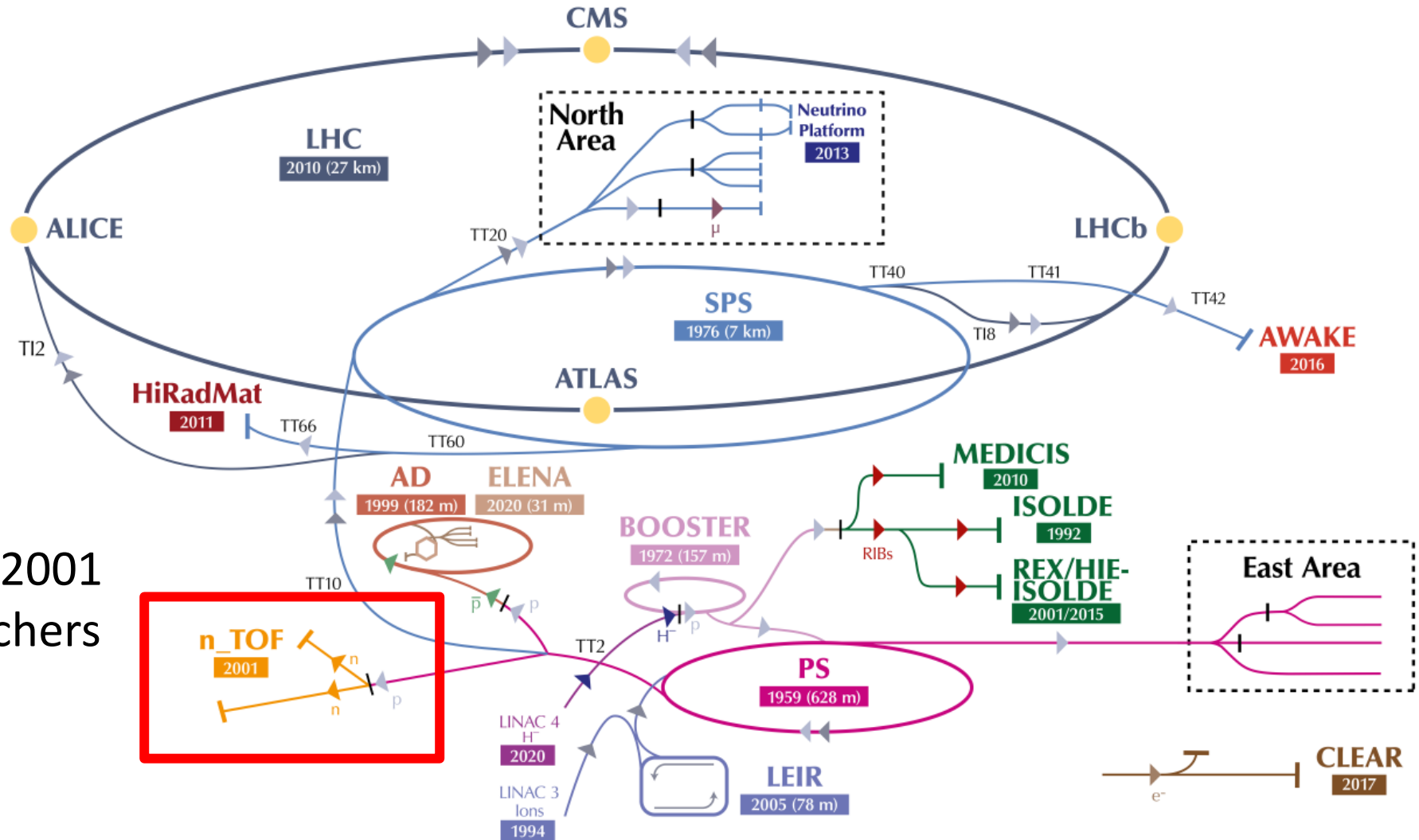
**MACS<sub>30</sub>(<sup>50</sup>Cr) = 37.1(20) mb** → <6% unc.



P. Pérez-Maroto et al., “Neutron activation as benchmark for cross section evaluations: Demonstration through the MACS of <sup>50</sup>Cr for nuclear technology applications”, *Physics Letters B*, 2025, vol. 862, p. 139360

# III. $^{50,53}\text{Cr}$ time-of-flight measurement at EAR1-n\_TOF@CERN

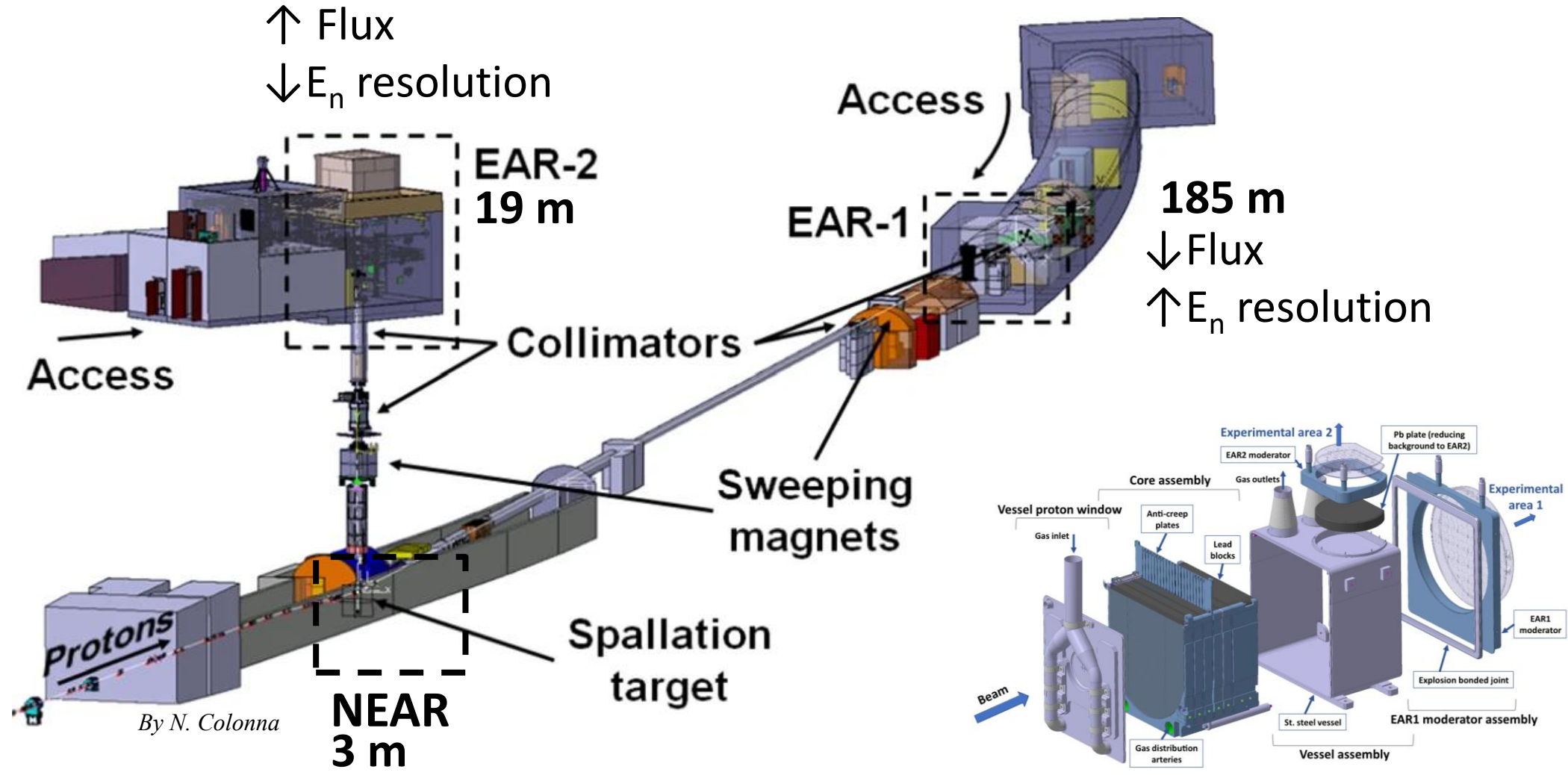
# The neutron Time-Of-Flight facility at CERN



## n\_TOF@CERN

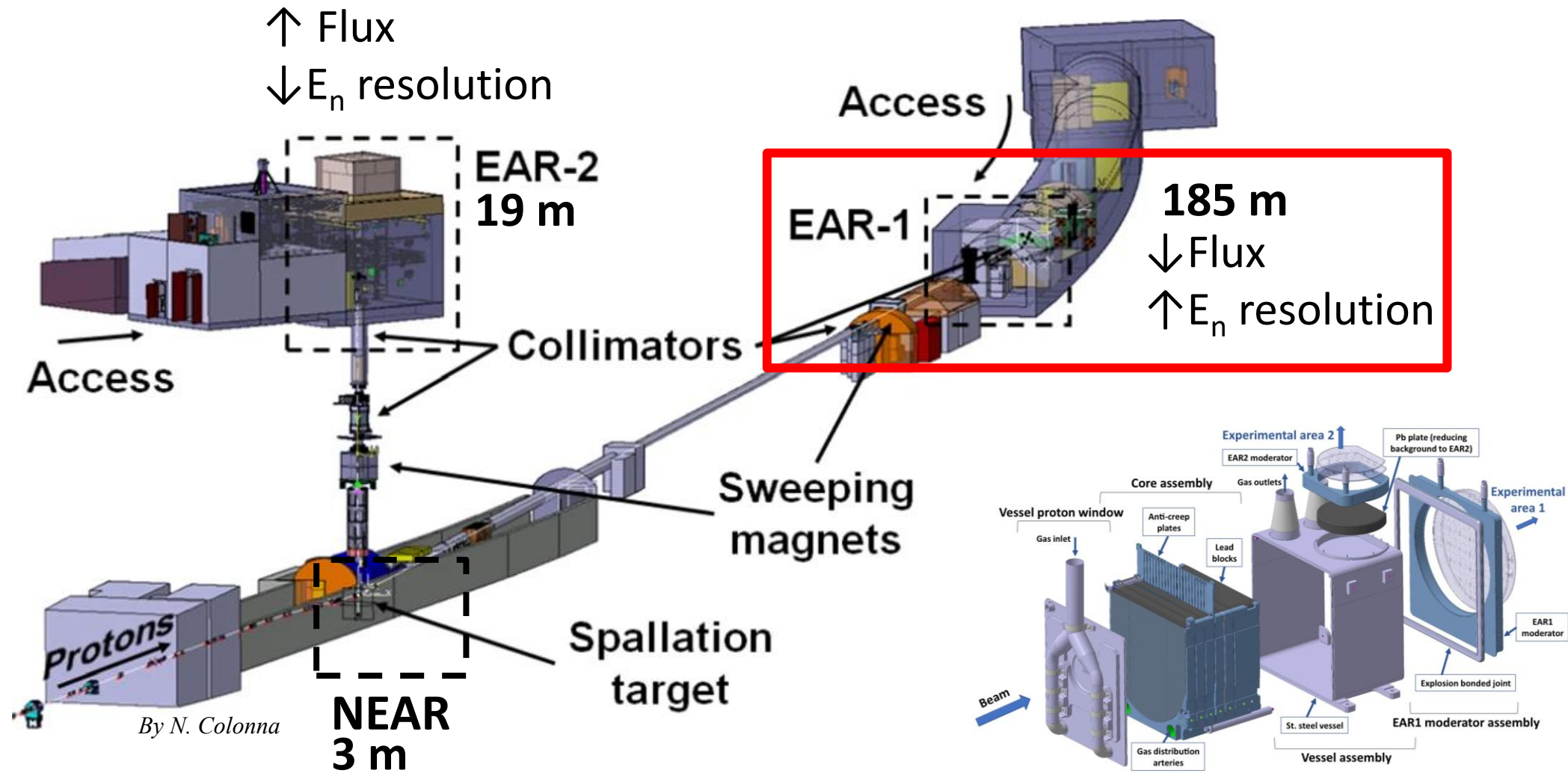
In operation since 2001  
 2026: ~150 researchers  
 from 42 institutes

# The neutron Time-Of-Flight facility at CERN



<https://ntof-exp.web.cern.ch>

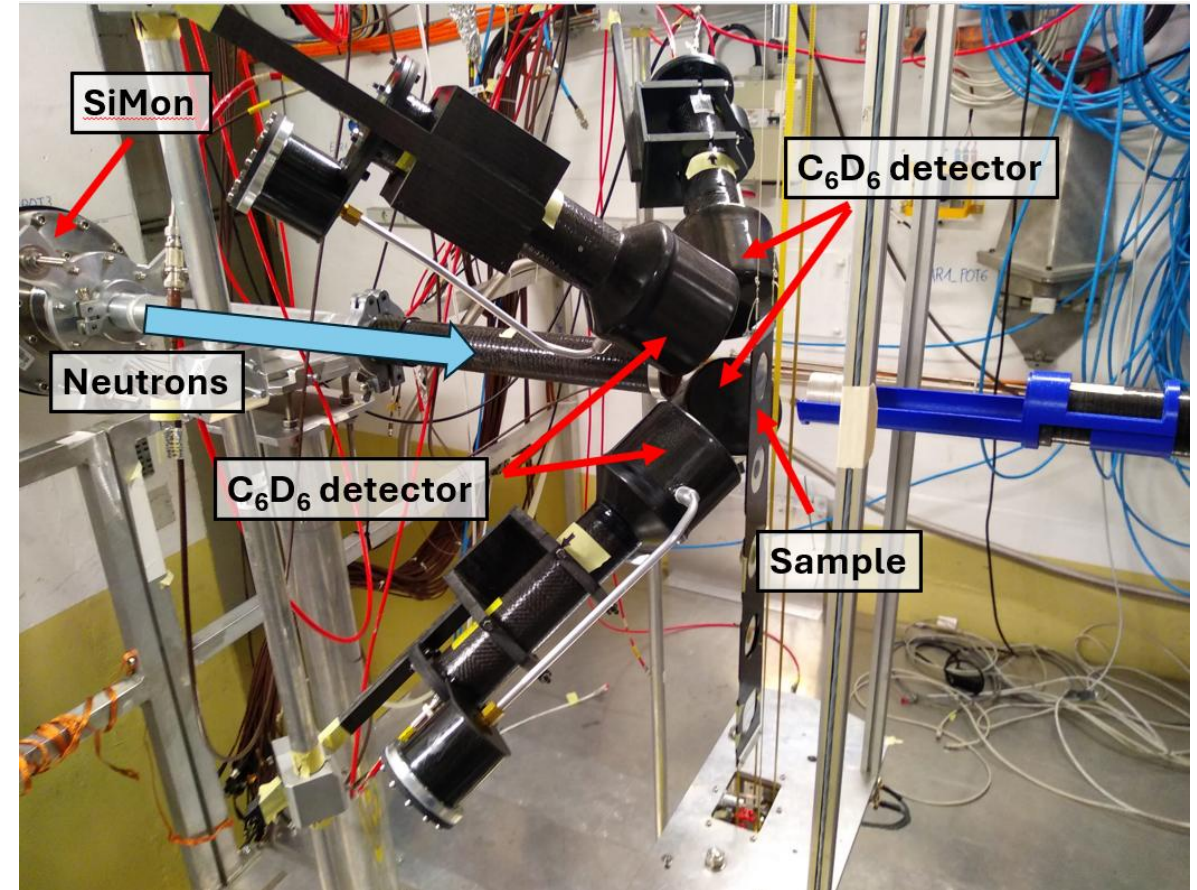
# The neutron Time-Of-Flight facility at CERN



<https://ntof-exp.web.cern.ch>

# Experimental set-up. C<sub>6</sub>D<sub>6</sub> TED detectors

- 4 C<sub>6</sub>D<sub>6</sub> TED detectors<sup>†</sup> at 8 cm and 125° from the sample.
- Developed specifically for n\_TOF.
- Made of carbon fiber.
- Main advantages:
  - Very low neutron sensitivity
  - Very fast response and time resolution
- TED → Pulse Height Weighting Technique.

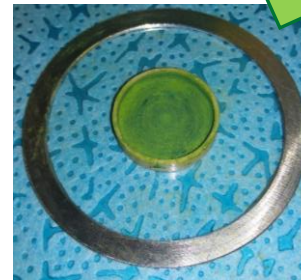
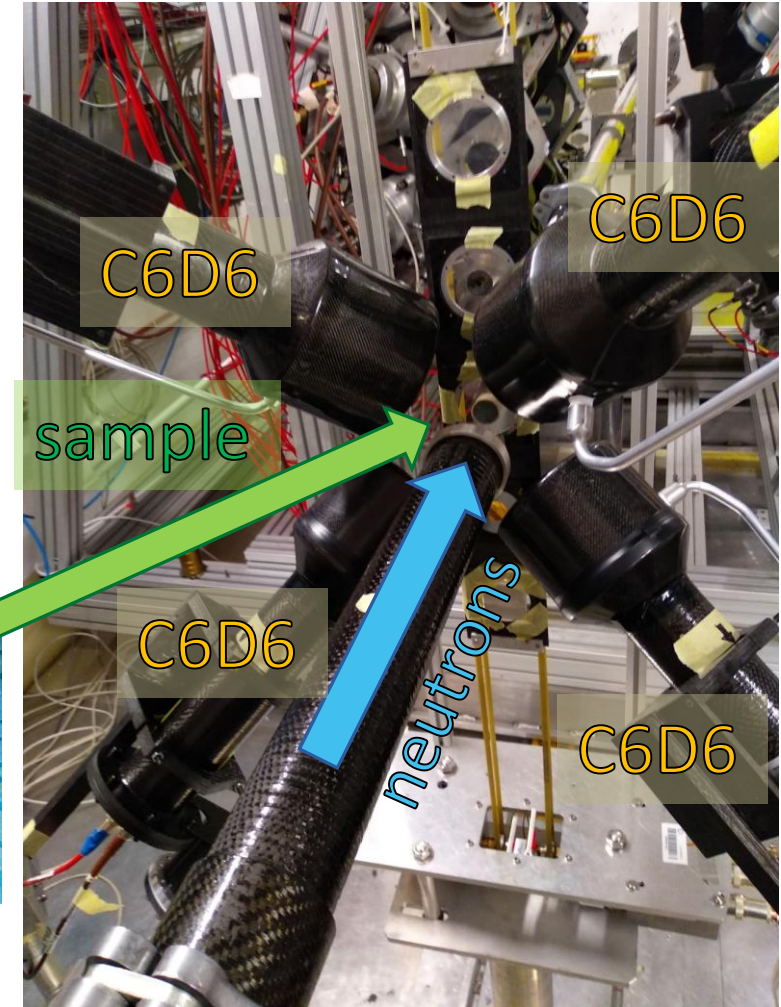


<sup>†</sup>R. Plag et al., “An optimized C<sub>6</sub>D<sub>6</sub> detector for studies of resonance-dominated (n,γ) cross-sections”, Nucl. Inst. & Meth. in Phys. Res. A 496 (2003)

# Experimental set-up. Samples

- The strategy is to use **two samples** for each isotope.
- 94.6(4)% of  $^{50}\text{Cr}$  and 97.7(2)% of  $^{53}\text{Cr}$ .

Experiment	Stieglitz (1971)	Beer (1975)	Kenny (1977)	Brusegan (1986)	Guber (2011)	This work (2024)
<u>Thickness <math>^{50}\text{Cr}</math></u> ( $10^{-3}$ at/barns)	8	18	5/8	7	-	<b>0.6/1.9</b> → x0.1
<u>Thickness <math>^{53}\text{Cr}</math></u> ( $10^{-3}$ at/barns)	14	14	8/12	12/60	14	<b>1.2/5.9</b> → x0.1



- Thin samples (1-10 keV) → MS effects under control
- Thick samples (10-100 keV) → Better statistics

## Thinnest samples ever measured

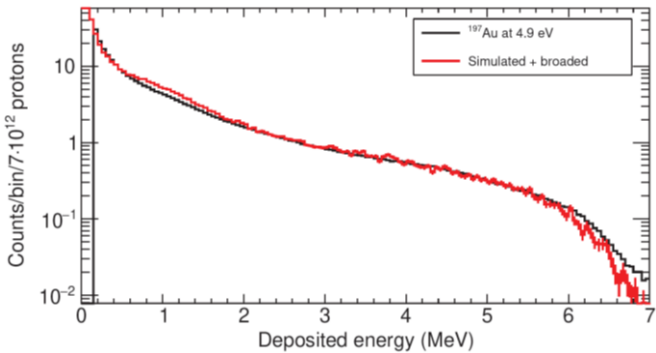
Plus ancillary samples... →

42 days long campaign  
750·10<sup>3</sup> protons pulses

# Capture yield determination

$$Y(E_n) = F_{corr} \frac{C_w(E_n) - B_w(E_n)}{F_{BIF} \cdot \varepsilon_c \cdot \Phi(E_n)}$$

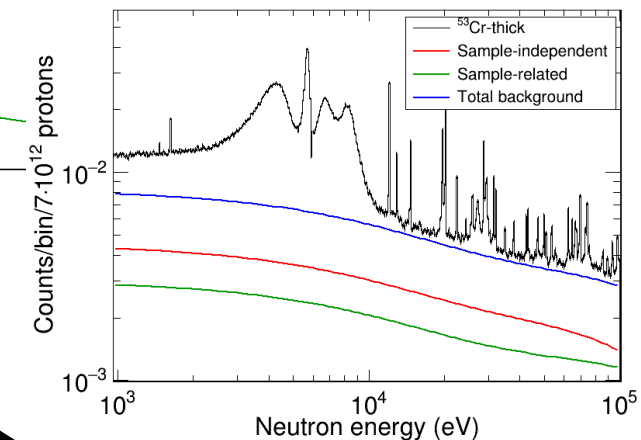
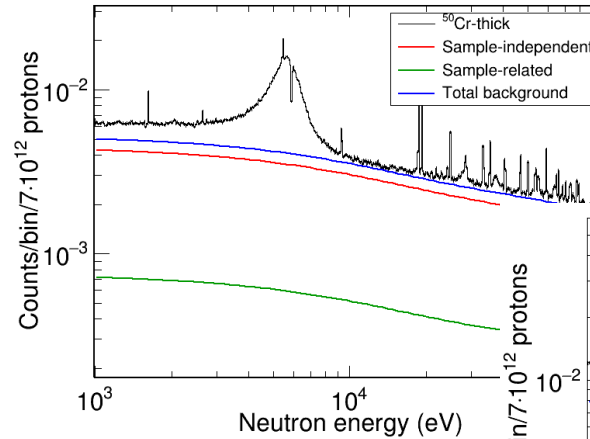
# Capture yield determination



$E_{thr} = 150 \text{ keV}$

Threshold correction factor

Total weighted counts



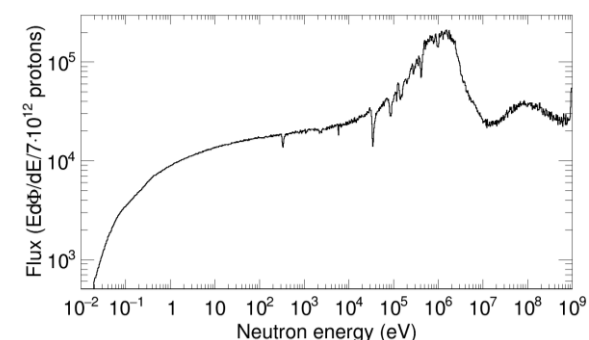
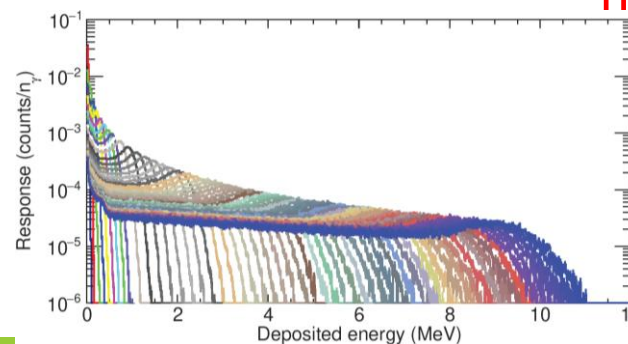
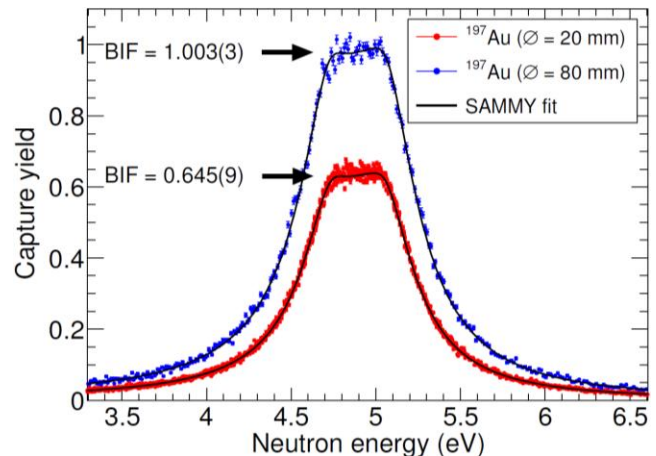
Background weighted counts

$$Y(E_n) = F_{corr} \frac{C_w(E_n) - B_w(E_n)}{F_{BIF} \cdot \epsilon_c \cdot \Phi(E_n)}$$

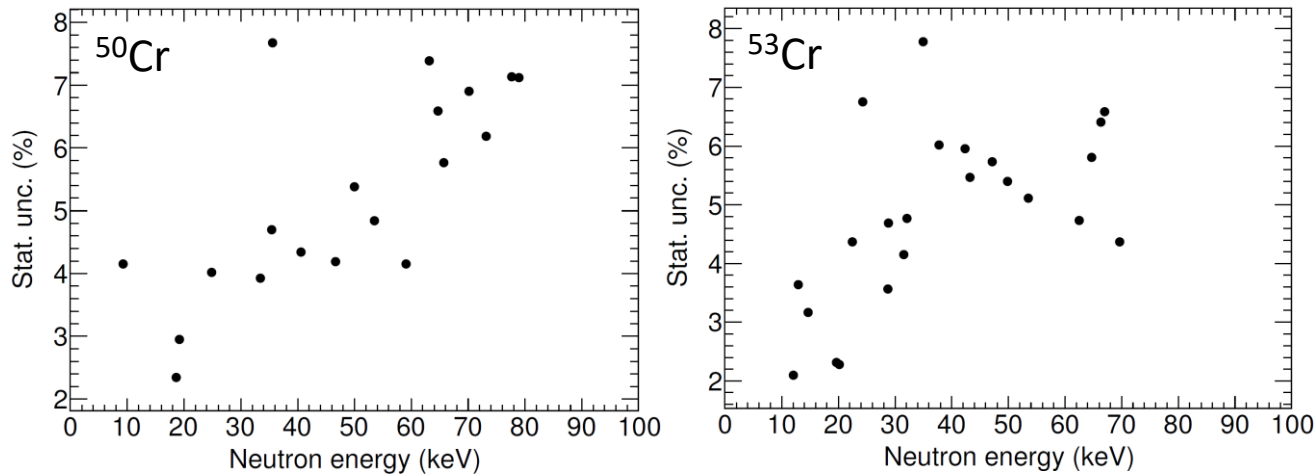
Beam Interception Factor (SRM)

Efficiency (PHWT)

Evaluated neutron flux



# Capture yield systematic uncertainties

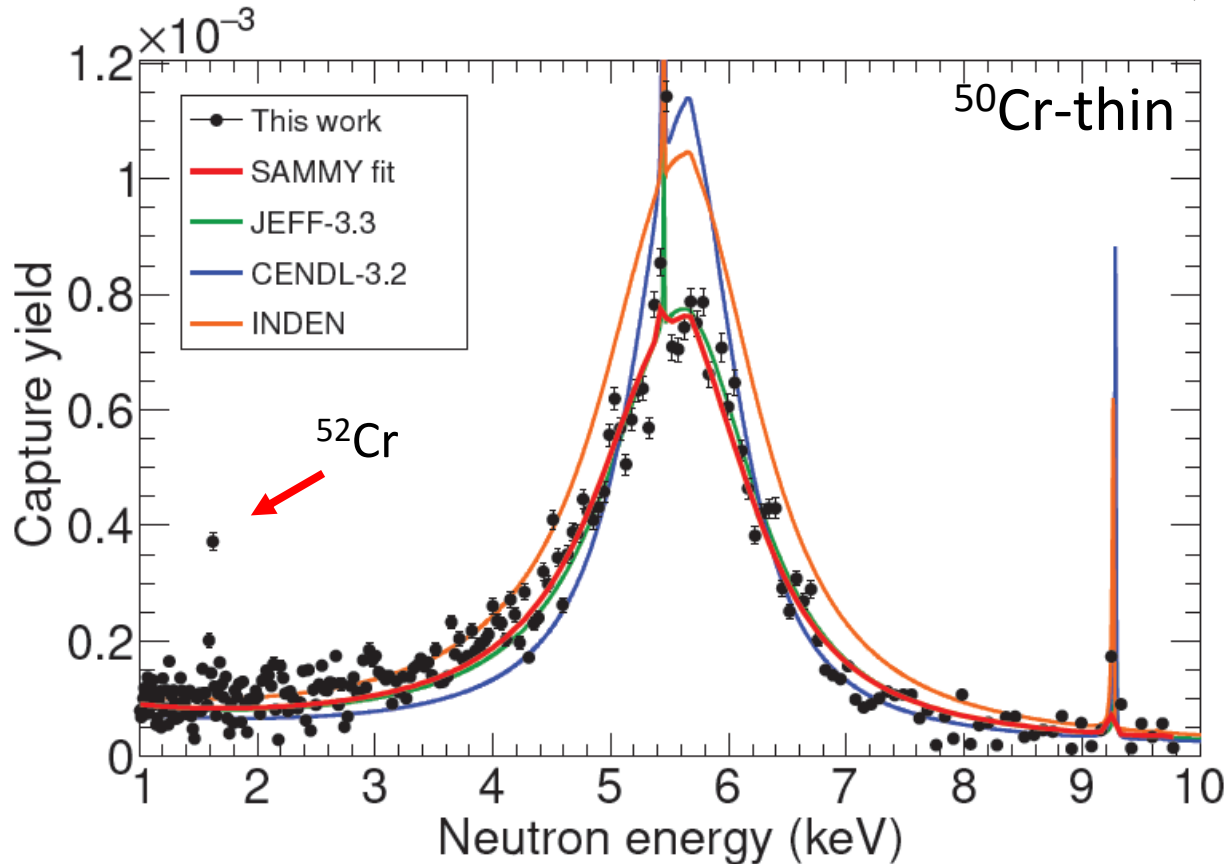


- A new methodology to apply the PHWT was implemented, which adds a source of uncertainty associated to the resonance total counts.
- In overall, the uncertainty remains below 9%, thus **fulfilling the NEA requirements.**

Contribution	Syst. Unc. (%)	
	<sup>50</sup> Cr	<sup>53</sup> Cr
Sample thickness	0.4	0.2
Monitor norm.	2.5	2.5
Neutron flux shape	2	2
Saturated res. norm.	1.5	1.5
Sample alignment	2	2
PHWT implementation	1.7	1.7
Cr cascades $\otimes f_{thr}$	1	1
RWF $\otimes$ statistics	2.3 - 7.7	2.1 - 7.8
<b>Overall (1-10 keV)</b>	<b>4.5</b>	<b>4.5</b>
<b>Overall (10-100 keV)</b>	<b>5.1 - 9.0</b>	<b>5.0 - 9.0</b>

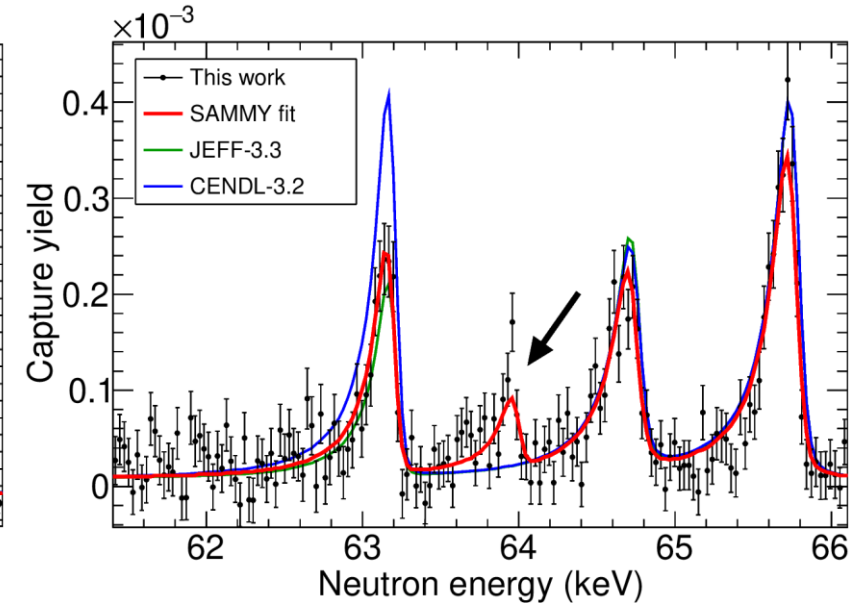
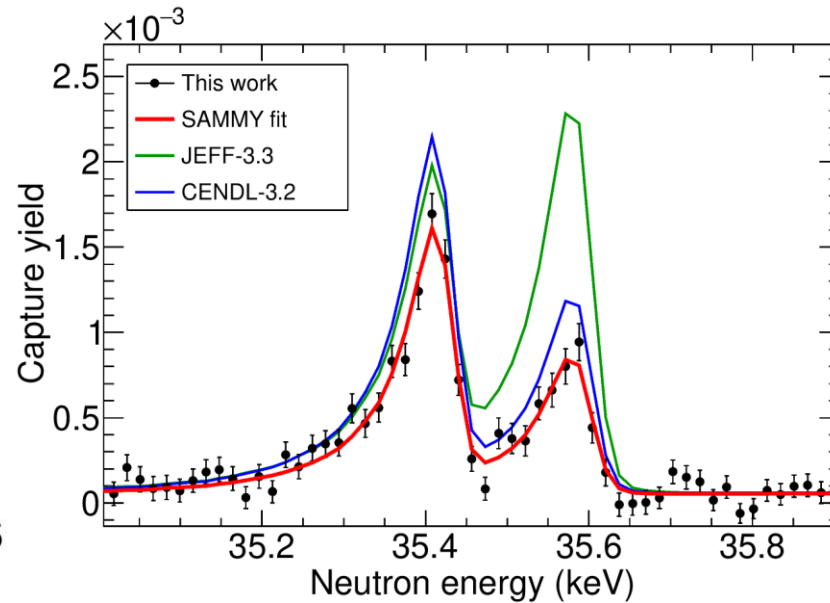
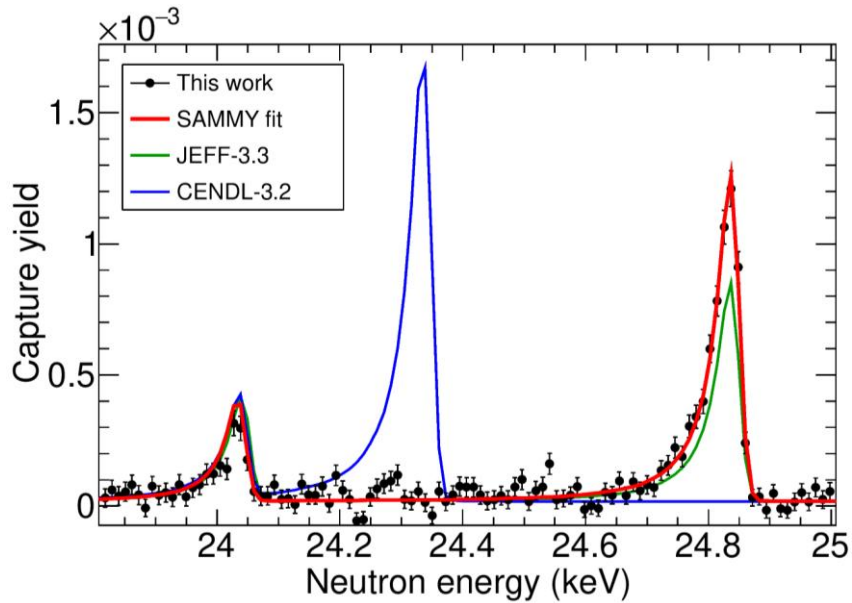
# Resonance analysis with SAMMY ( $^{50}\text{Cr}$ )

- Main resonance  $\rightarrow$  in agreement with JEFF-3.3 (even  $K_\gamma$  also similar to CENDL-3.2).
- Overestimation by INDEN.
- Previous energy shifted: from  $E_n = 5.621$  keV to  $E_n = 5.581(6)$  keV  $\rightarrow$  Multiple-scattering effects



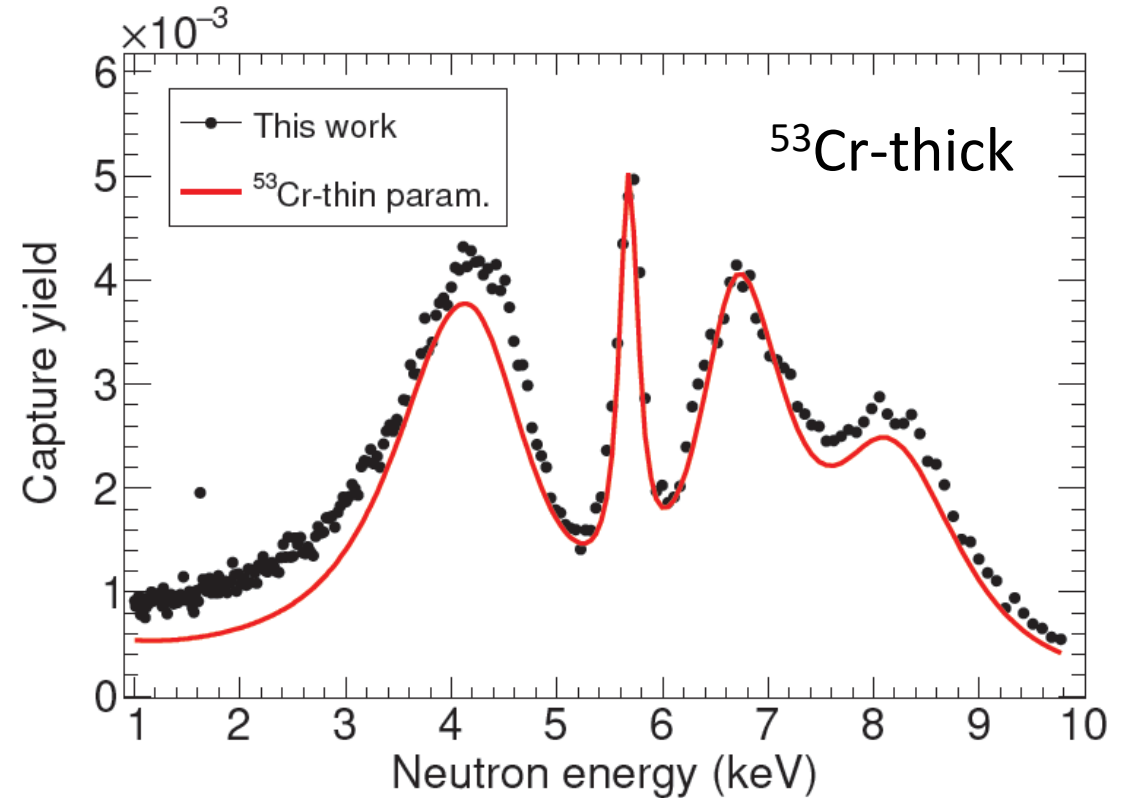
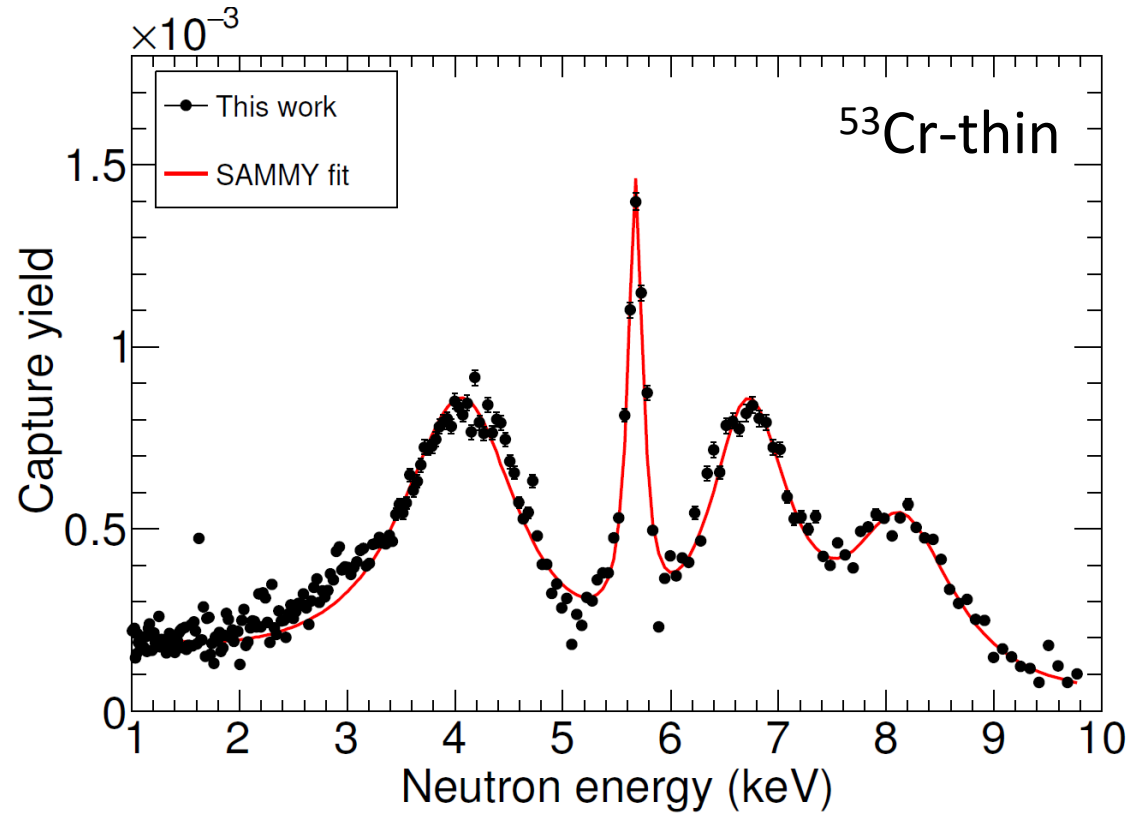
# Resonance analysis with SAMMY ( $^{50}\text{Cr}$ )

- For  $E_n > 10$  keV, INDEN adopts the same parameters than JEFF-3.3
- 33 resonances described.
- 3 of them removed from JEFF-3.2, but visible in our data (for example at 64 keV).



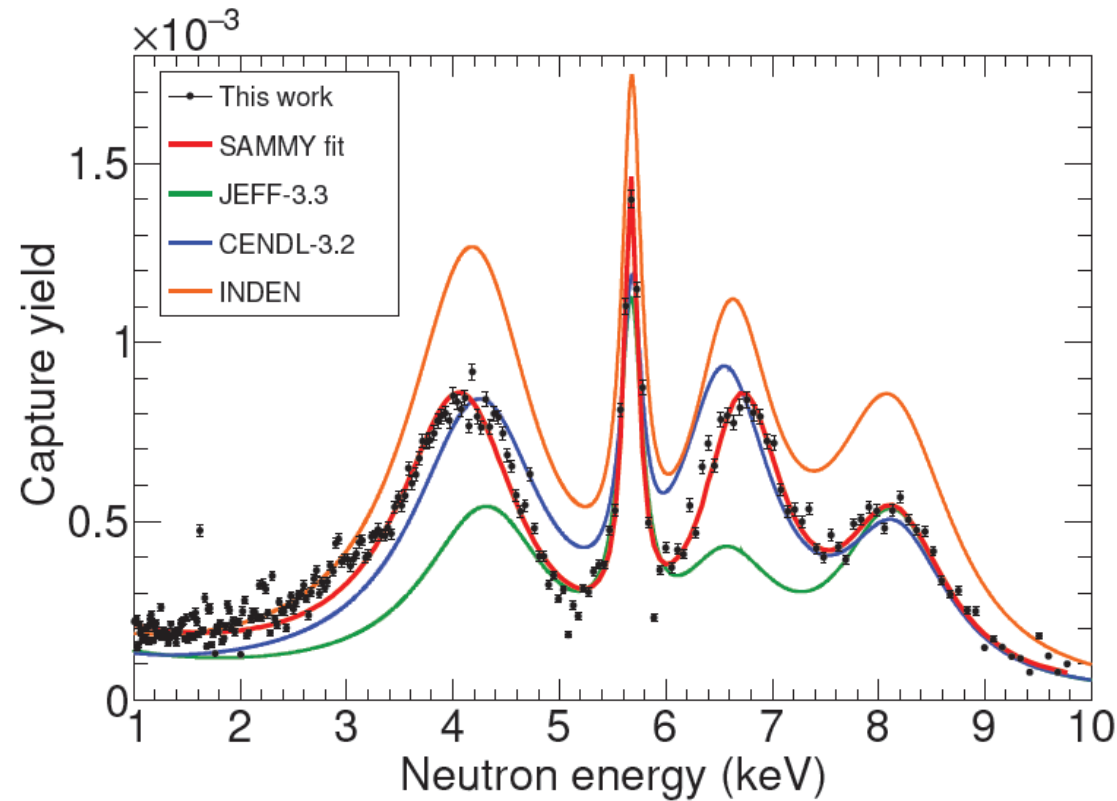
# Resonance analysis with SAMMY ( $^{53}\text{Cr}$ )

- The MS effects are very large  $\rightarrow$   $\sim 7\text{mm}$  thickness.
- SAMMY fails to accurately evaluate the very strong MS effects.



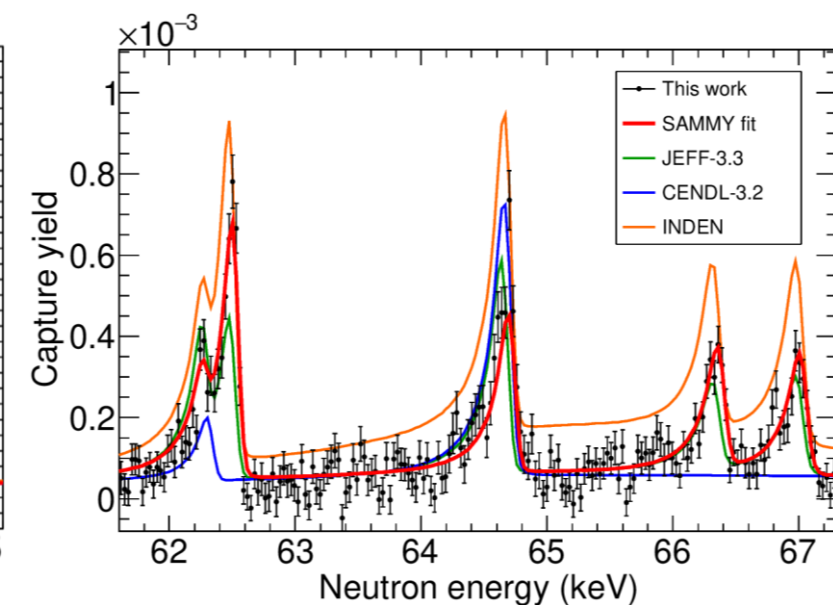
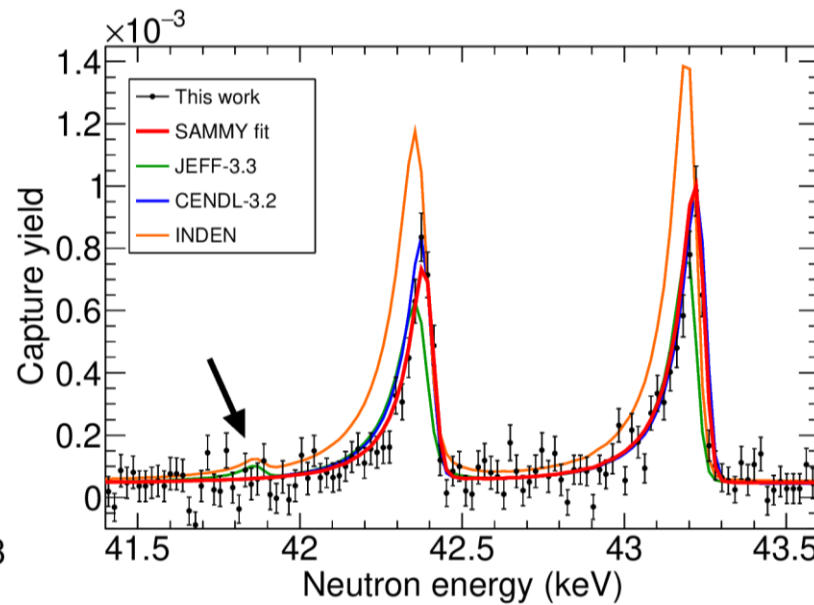
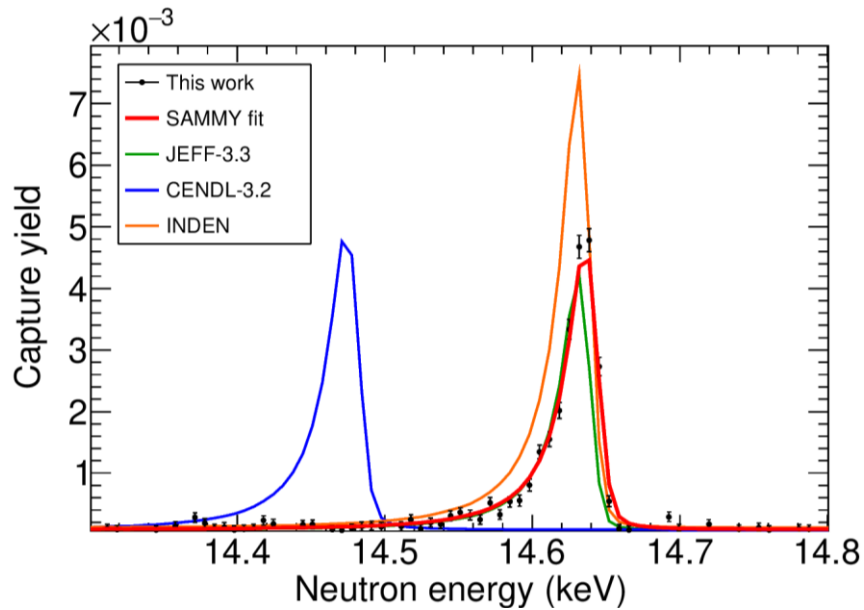
# Resonance analysis with SAMMY ( $^{53}\text{Cr}$ )

- The MS effects are very large  $\rightarrow$   $\sim 7\text{mm}$  thickness.
- SAMMY fails to accurately evaluate the very strong MS effects.
- Our data is much closer to CENDL-3.2 (still with differences).



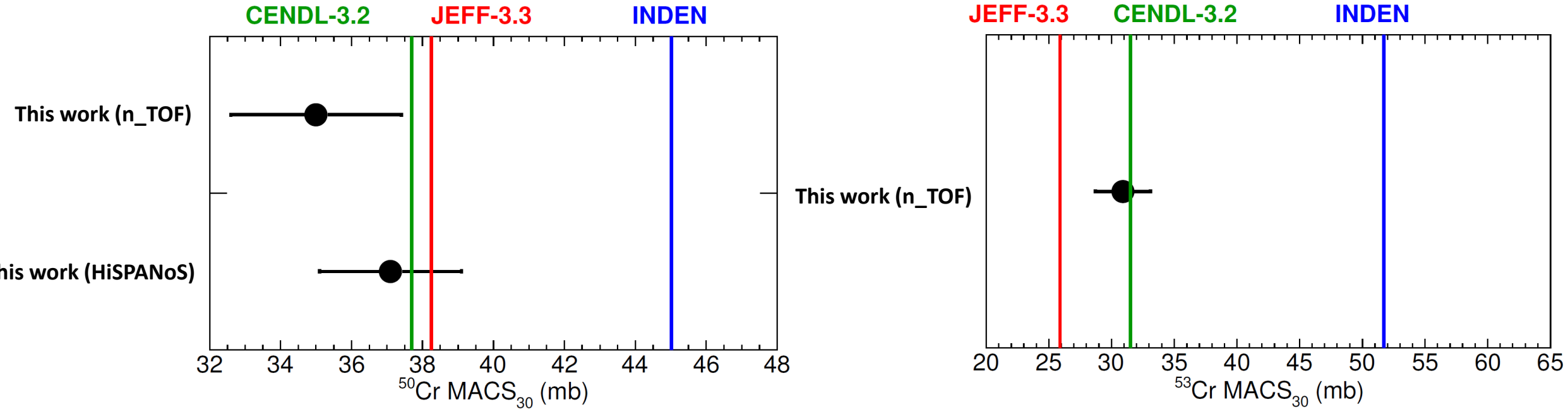
# Resonance analysis with SAMMY ( $^{53}\text{Cr}$ )

- More differences between evaluations than in  $^{50}\text{Cr}$ .
- A total of 51 resonances have been described.
- Some of them (included in JEFF-3.3 and INDEN) are not visible in our data.
- In general, INDEN seems to overestimate the capture cross section.



# $^{50,53}\text{Cr}(n,\gamma)$ at EAR1 results

MACS<sub>30</sub> extracted from n\_TOF ( $E_n < 100$  keV) + evaluations above 100 keV.



- Results for  $^{50}\text{Cr}$  and  $^{53}\text{Cr}$  are 20% and 70% lower than INDEN, respectively.
- $^{50}\text{Cr} \rightarrow \text{MACS}_{30}$  from HiSPANoS and n\_TOF are compatible within uncertainty.

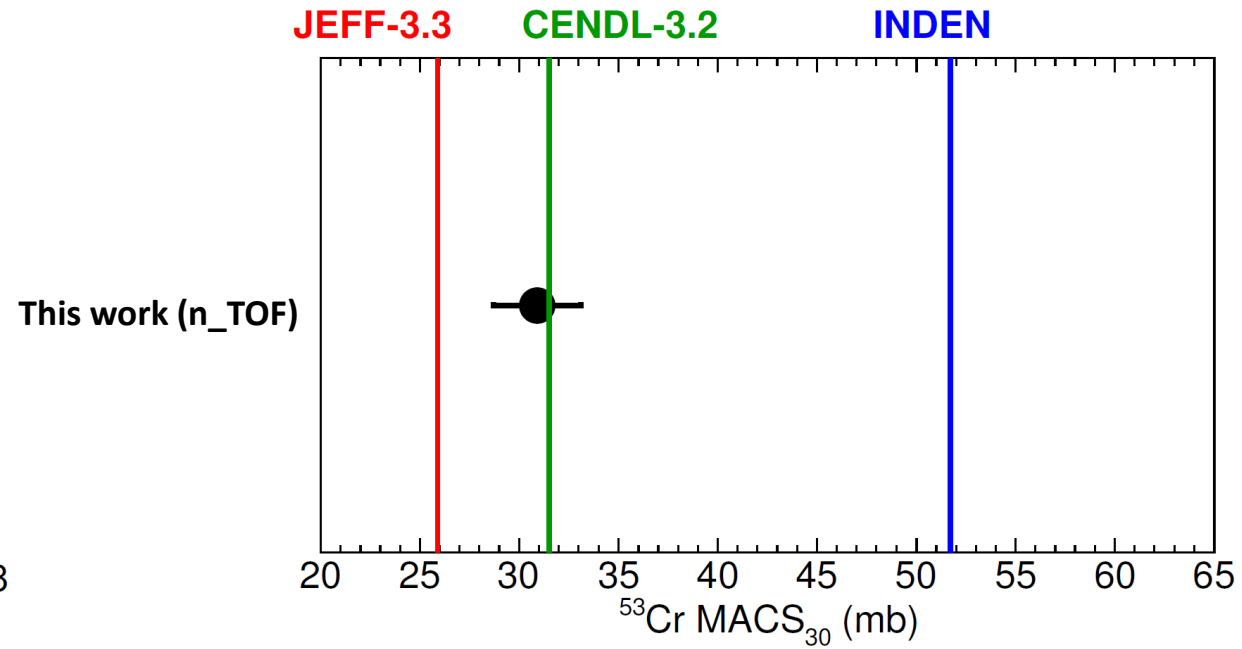
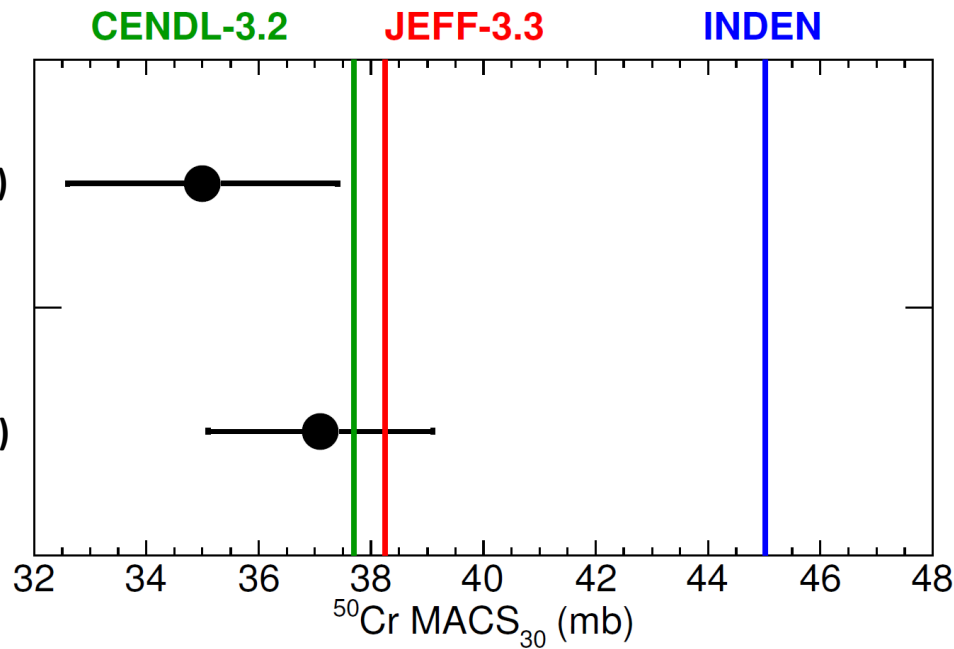
P. Pérez-Maroto et al., “**New measurement  $^{50}\text{Cr}$  and  $^{53}\text{Cr}$  (n,γ) cross sections at n\_TOF: a call for chromium nuclear data revision**”, *The European Physical Journal A*, 2026, vol. 62(1), p. 5

# IV. Summary & Conclusions

# Summary & Conclusions

- A clear goal: improving the  $^{50,53}\text{Cr}(n,\gamma)$  cross section to 8-10% accuracy at 1-100 keV.
  - Two experiments:
    - $^{50}\text{Cr}$  activation at HiSPANoS@CNA.
    - $^{50,53}\text{Cr}$  ToF at n\_TOF@CERN.
- }

  - Uncertainties within the objective.
  - Both cross sections clearly lower than INDEN.
  - Both experiments are compatible.



# Thank you for your attention

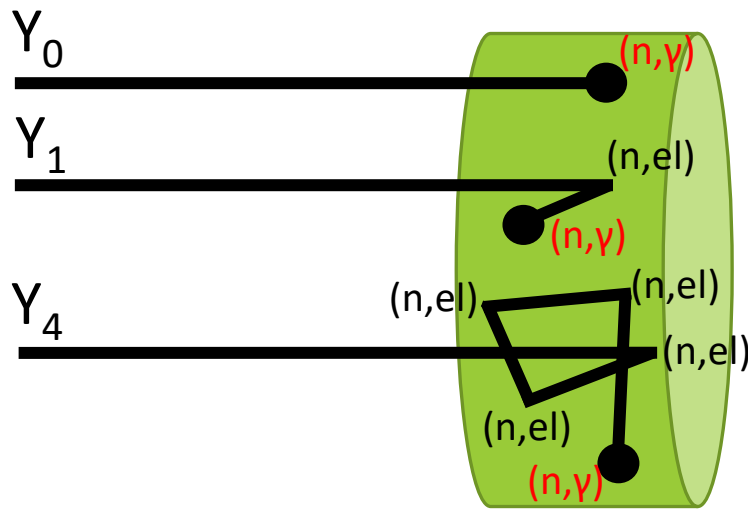
Pablo Pérez Maroto - [pperezma@cern.ch](mailto:pperezma@cern.ch)

Acknowledgements: Euroatom research and training programme 2014-2018 under grant agreement No 847594 (ARIEL). Spanish national projects RTI2018-098117-B-C21, PID2019-104714GB-C22, PID2021-123879OB-C21 and PID2022-138297NB-C22 funded by MCIN/AEI/10.13039/501100011033 and by "ERDF A way of making Europe". FPI national Grant No PRE2019-089678. Recovery & Resilience Facility (Spain). The European Union – NextGenerationEU.



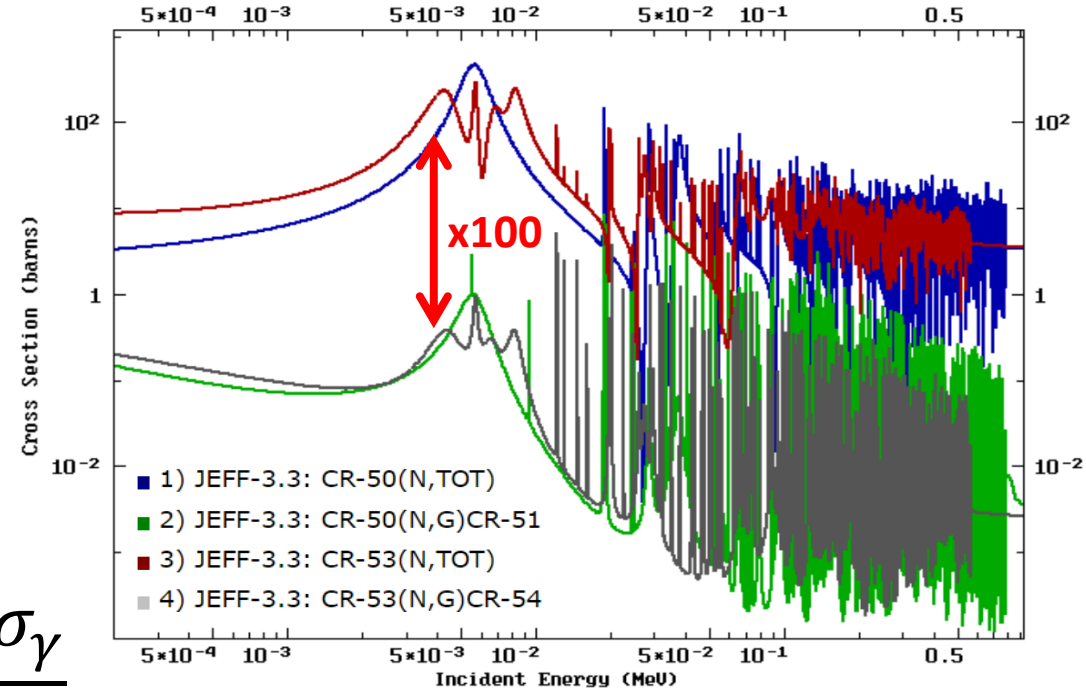
# Backup. Why the discrepancies?

- The main problem for measuring  $\text{Cr}(n,\gamma)$  is the large neutron multiple-scattering effects
- In the previous measurements thick samples were used, aiming for good statistics in a very wide energy range



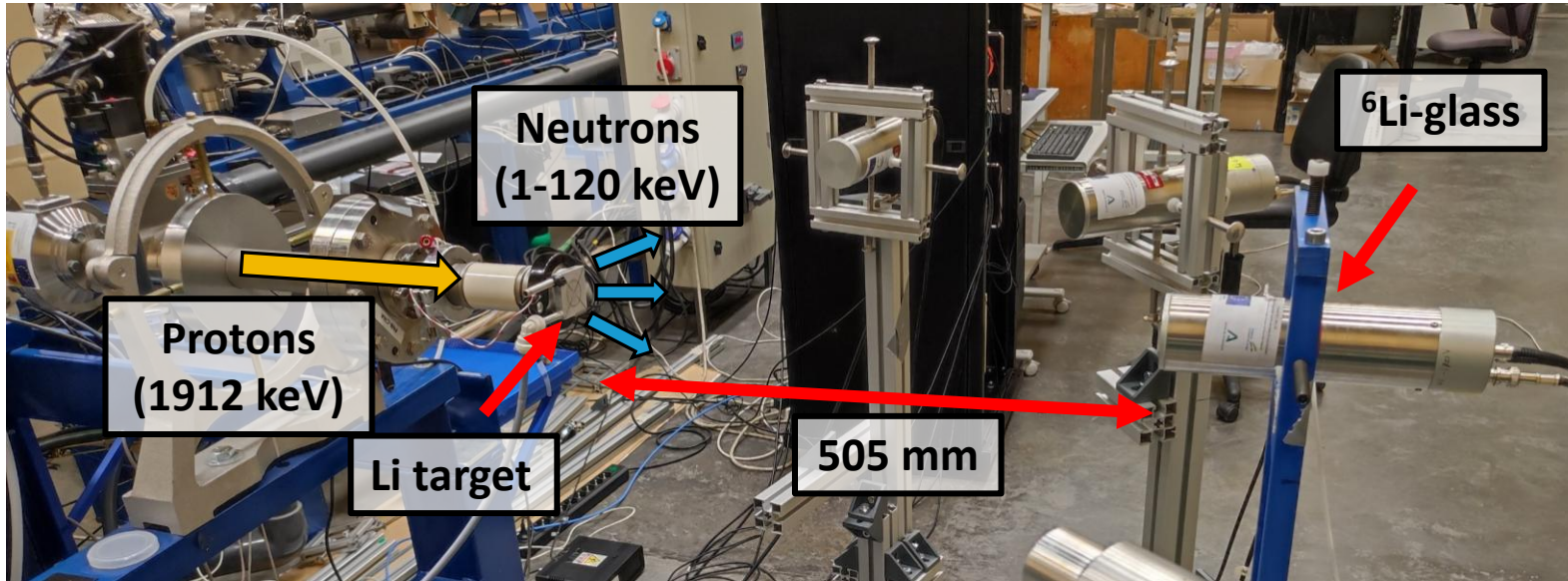
$$Y_0 = (1 - e^{-n\sigma_t}) \frac{\sigma_\gamma}{\sigma_t}$$

Capture yield (captures/neutron)  $\rightarrow Y = \underbrace{Y_0}_{\text{Analytical (accurate)}} + \underbrace{Y_1 + Y_2 + Y_3 \dots}_{\text{Numerical (approximate)}}$

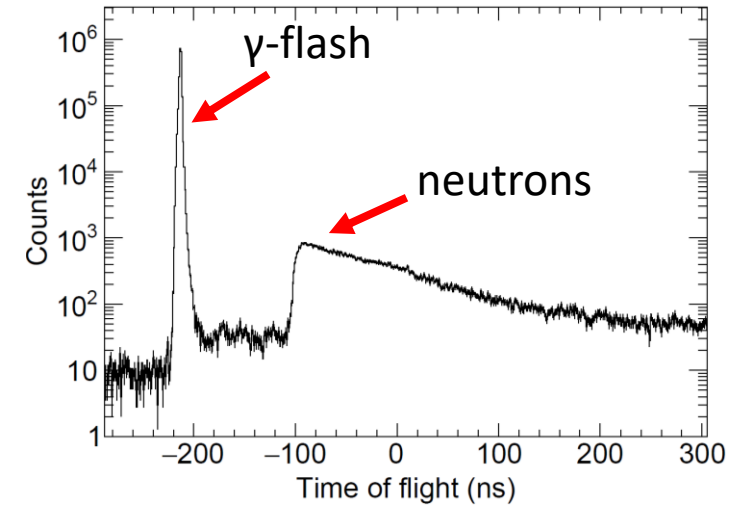


# Backup. MB spectrum: ToF characterization

A 30 keV quasi-Maxwellian spectrum can be produced by  ${}^7\text{Li}(p,n)$  with  $E_p=1912\text{ keV}^\dagger$ .



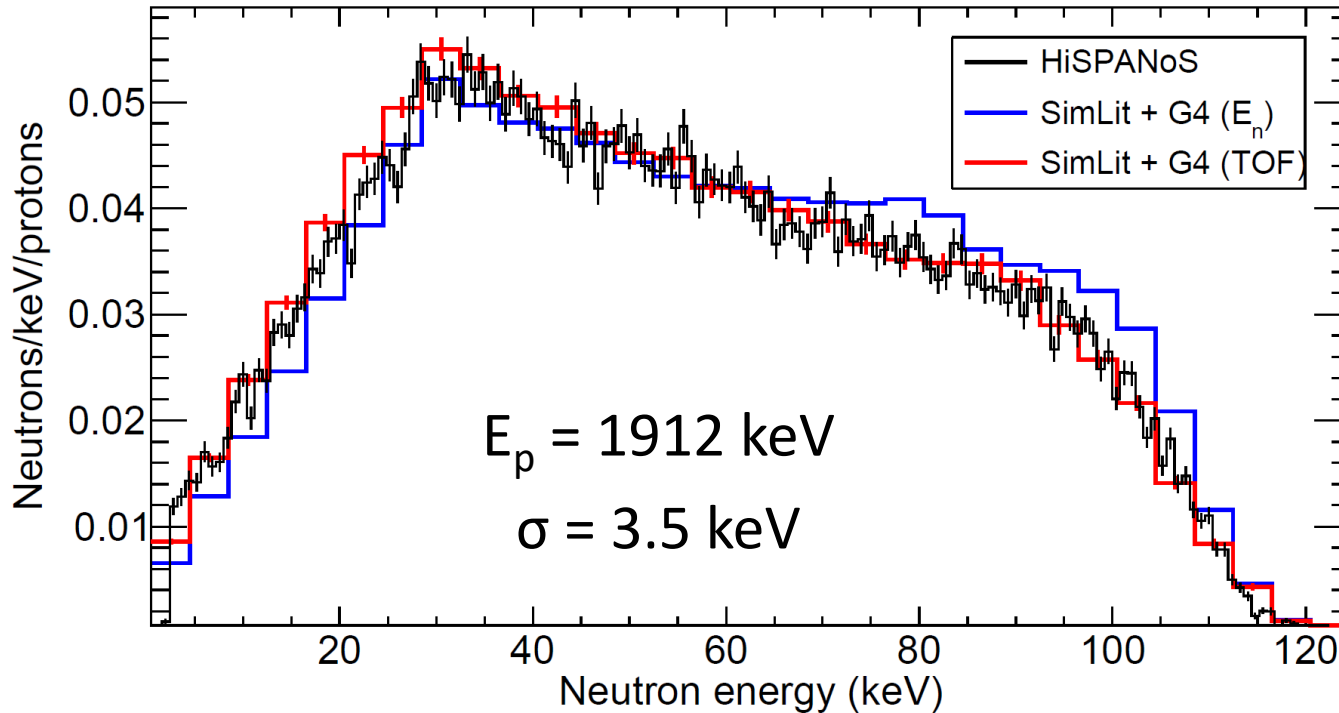
Li-glass detectors  $\rightarrow$  based on the  ${}^6\text{Li}(n,\alpha){}^3\text{H}$  reaction



$^\dagger$ W. Ratynski & F. Käppeler, “Neutron capture cross section of  ${}^{197}\text{Au}$ : A standard for stellar nucleosynthesis”, Physical Review C 37(2) (1988)

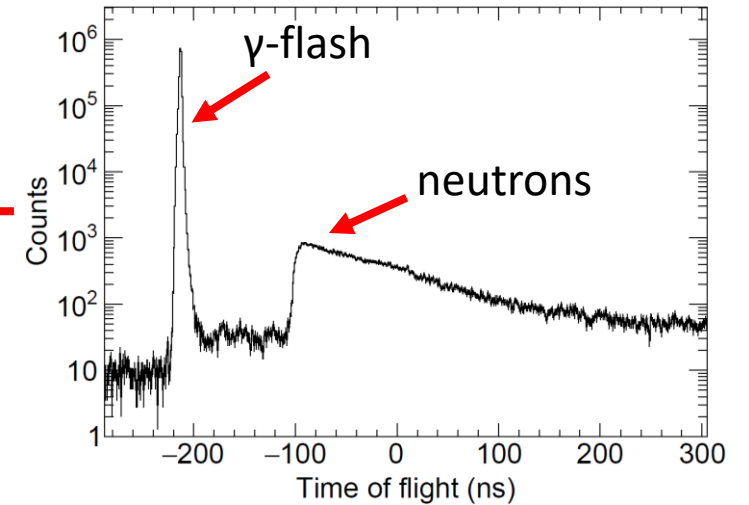
# Backup. MB spectrum: ToF characterization

The neutron field was characterized by time-of-flight + simulations.



$$E_n = \frac{K^2 L^2}{t^2}$$

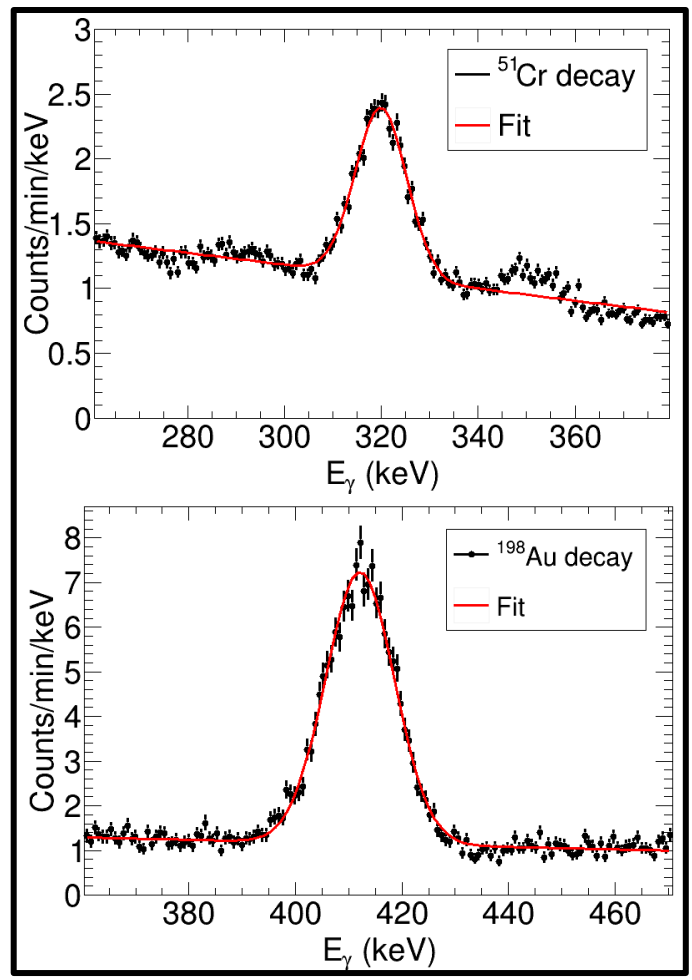
Li-glass detectors → based on the  ${}^6\text{Li}(n,\alpha){}^3\text{H}$  reaction



- SimLiT → Neutron production
- GEANT4 → Neutron transport

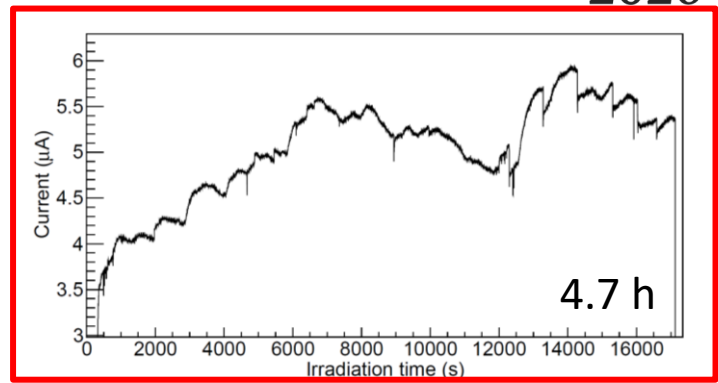
} The neutron field was characterized by time-of-flight + simulations.

# Backup. Neutron activation analysis



Counts → Gaussian + linear fit

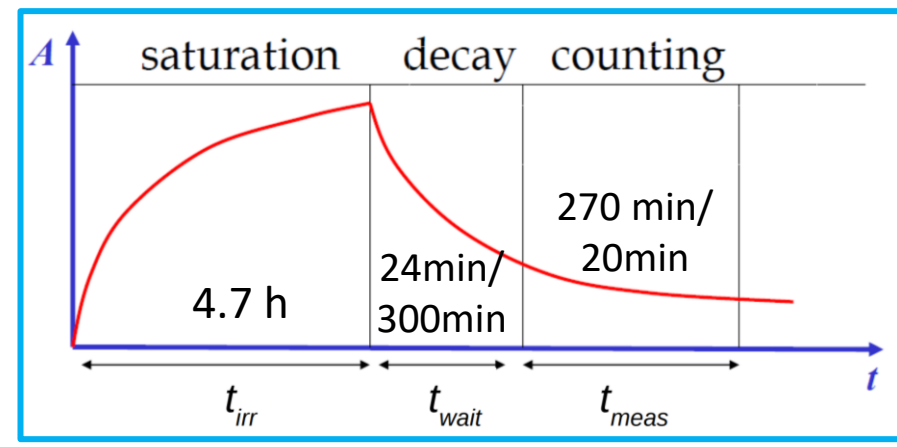
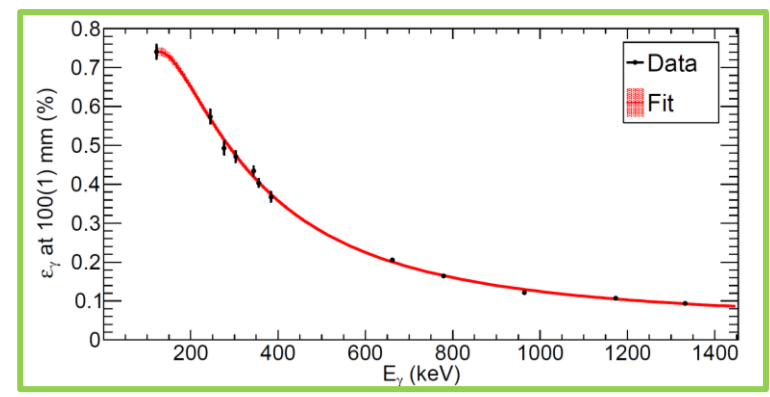
$$N_{act} = \frac{A_{EOI}}{\lambda} = \frac{\bar{C} \cdot e^{\lambda t_{wait}} \cdot f_{irr}}{\bar{I}_{\gamma} \cdot \epsilon \cdot (1 - e^{-\lambda t_{meas}})}$$



Decay during irradiation → current measurement

Decay during transport and measurement

Efficiency

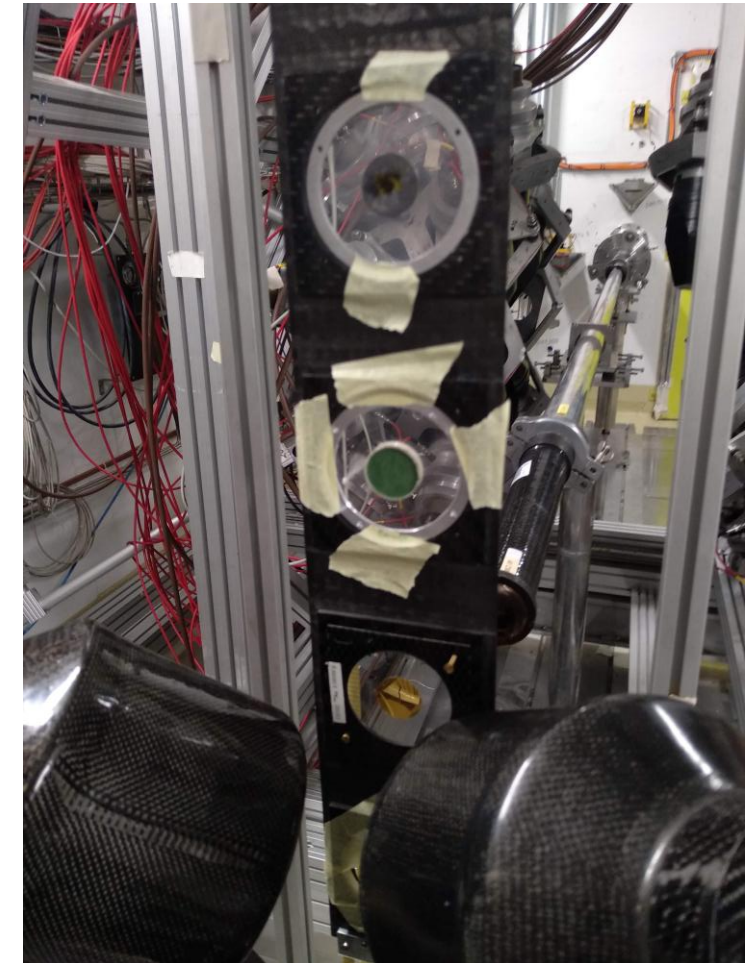


# Backup. Ancillary samples

Some ancillary measurements were performed during the experimental campaign

- Dummy (empty PEEK capsule)
  - Empty (empty aluminum ring)
  - 1 mm <sup>nat</sup>C (neutron-scattering)
  - 100 μm <sup>197</sup>Au (two diameters) → Normalization
- } → Background

Sample	Diameter (mm)	$n_{at}$ ( $10^{-3}at/b$ )
Dummy (2)	22	-
<sup>197</sup> Au	20	0.583
<sup>197</sup> Au	80	0.644
<sup>nat</sup> C	20	8.702

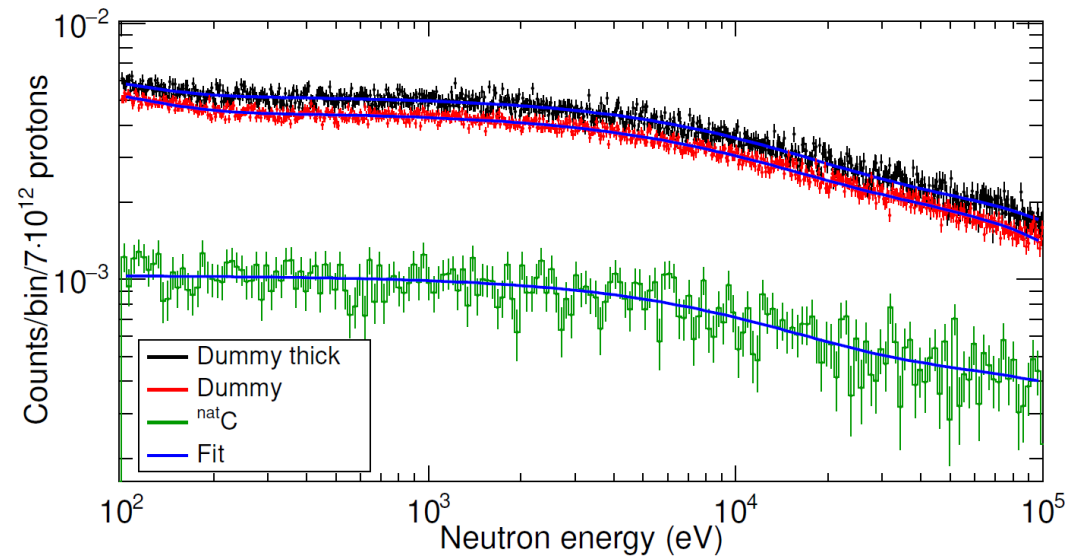
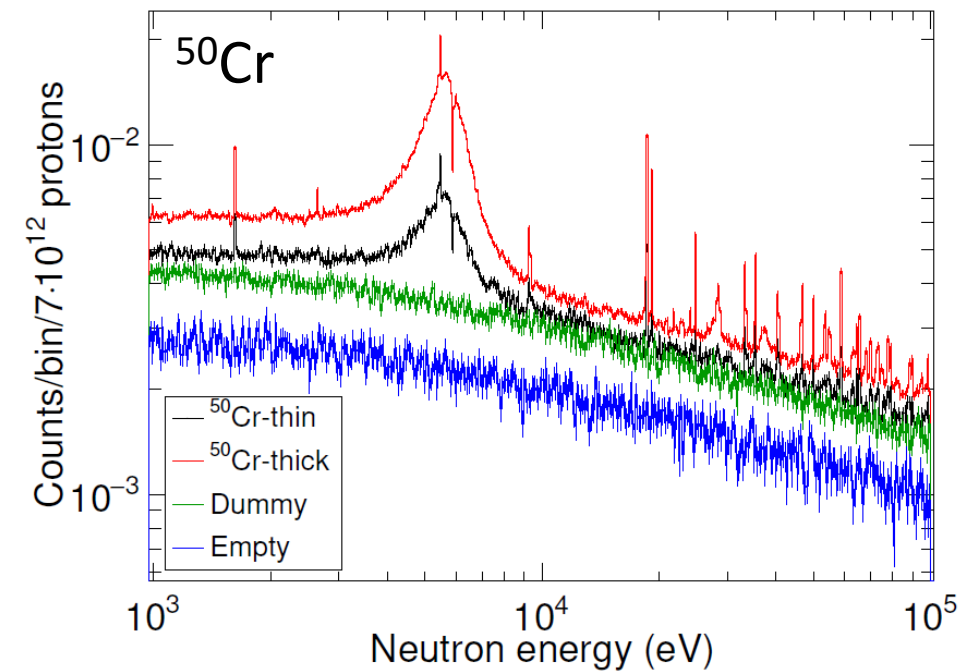


# Backup. Background determination

The background affecting the measurement can be divided in:

- Sample independent → Neutron-scattering and capture outside the sample: Dummy & Empty
- Sample related → Neutron-scattering **inside the sample**: natC

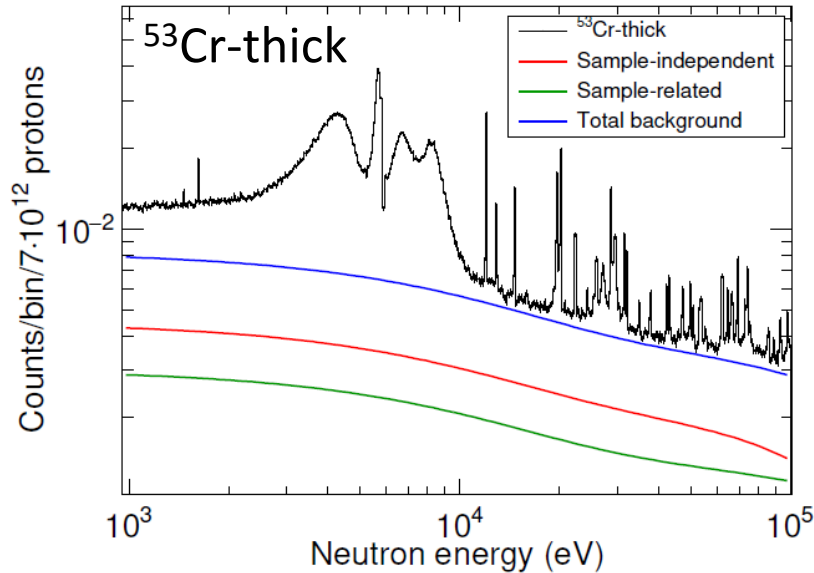
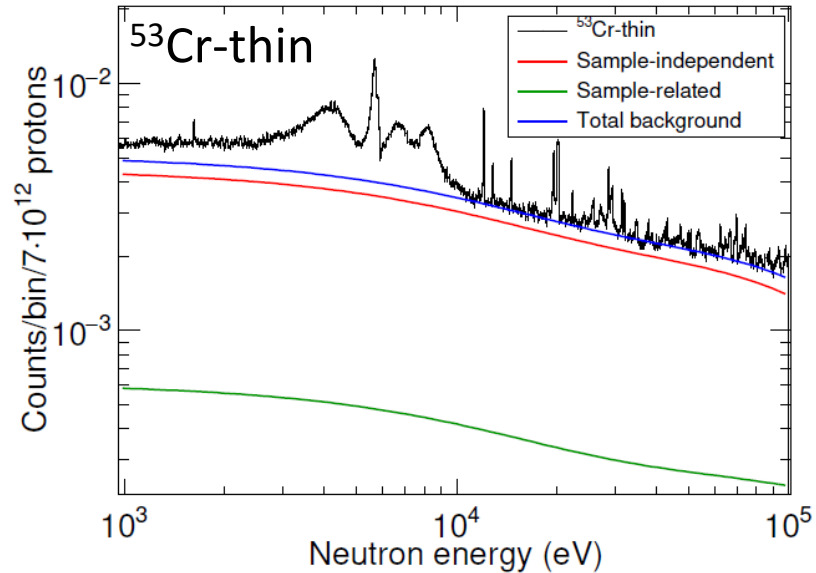
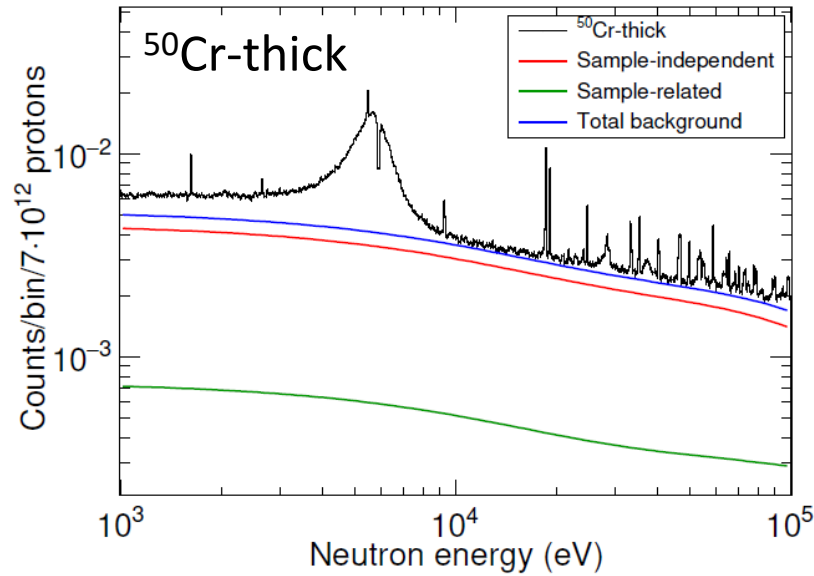
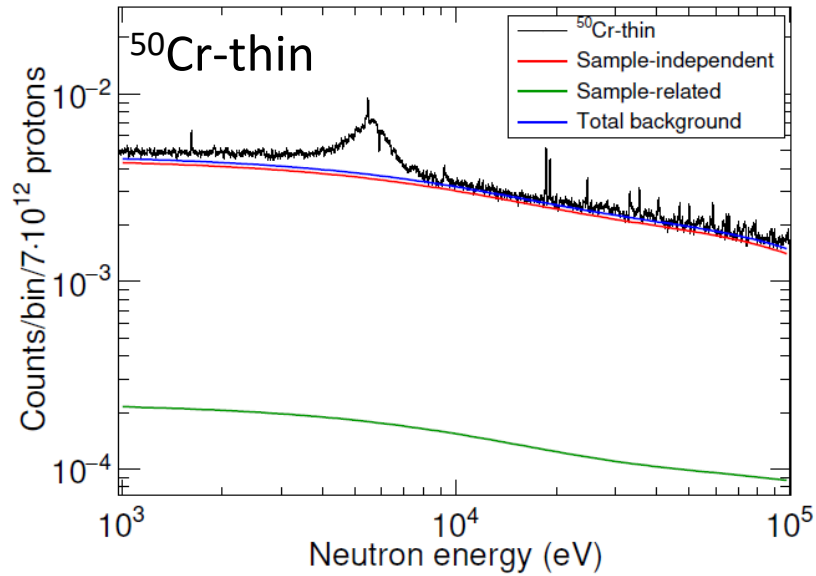
$$F_n = \left\langle \frac{\sigma_{el,Cr}}{\sigma_{el,C}} \right\rangle \frac{n_{at,Cr}}{n_{at,C}}$$



Sample	$F_n$
$^{50}\text{Cr}$ -thin	0.25
$^{50}\text{Cr}$ -thick	0.72
$^{53}\text{Cr}$ -thin	0.59
$^{53}\text{Cr}$ -thick	2.91

$$B(E_n) = a_0 + \sum_{i=1}^k b_i (1 - e^{-c_i E_n}) e^{-d_i E_n}$$

# Backup. Background determination

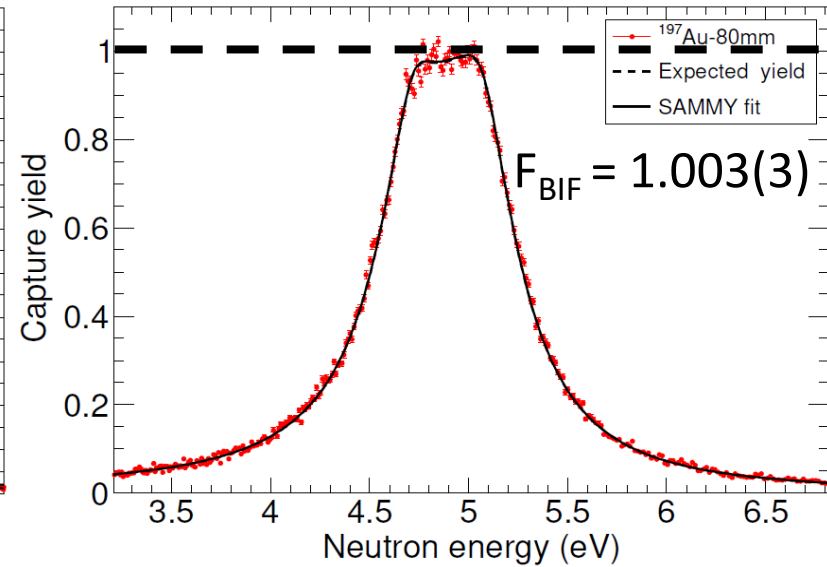
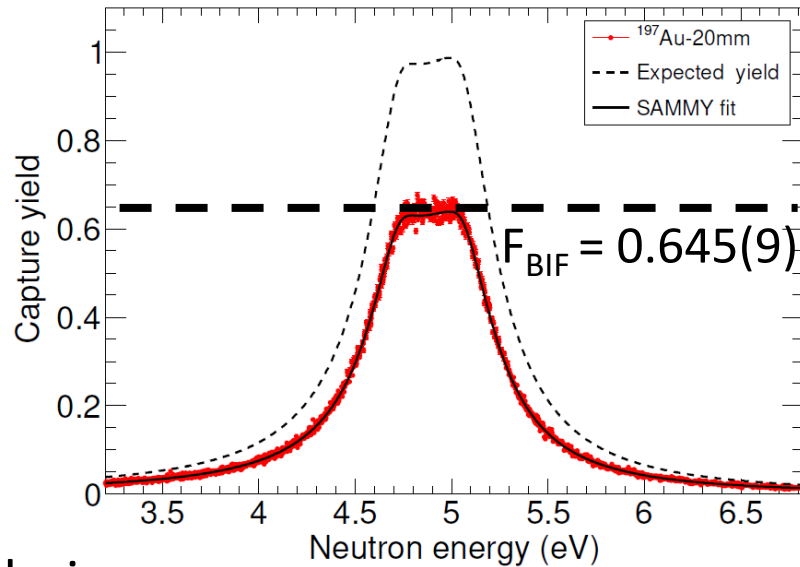
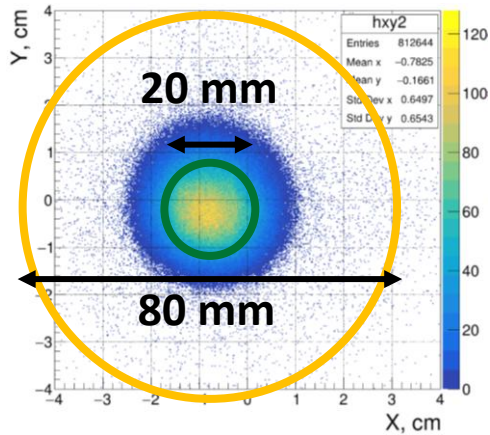


- Some background is still visible below the main resonance in the thick samples → Region not used.
- The residual background is included in the yield analysis.

# Backup. Capture yield normalization: SRM

The final step to obtain the capture yield is the normalization factor  $F_{\text{BIF}} \rightarrow {}^{197}\text{Au}$  sample

$$Y(E_n) = (1 - e^{-n\sigma_t}) \frac{\sigma_\gamma}{\sigma_t} \begin{cases} n_{\text{at}}\sigma_t \gg 1 \\ \sigma_t \approx \sigma_\gamma \end{cases} \rightarrow Y(E_n) \cong 1 \xrightarrow{\text{red arrow}} \text{Saturated Resonance Method (SRM)}^\dagger$$

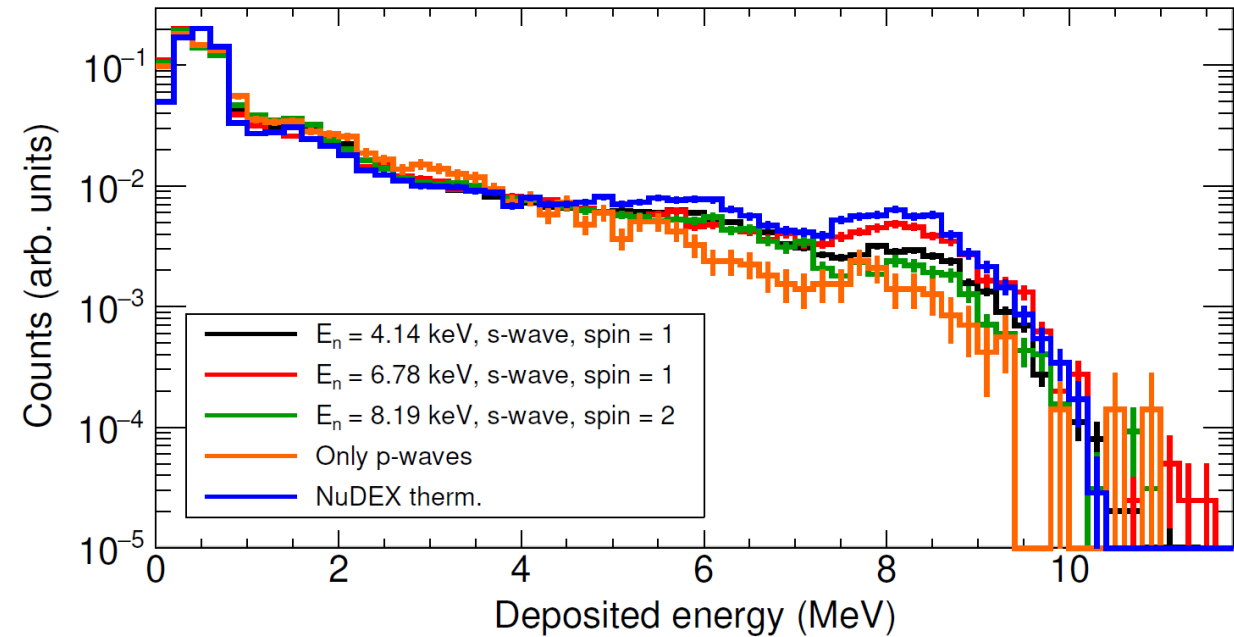
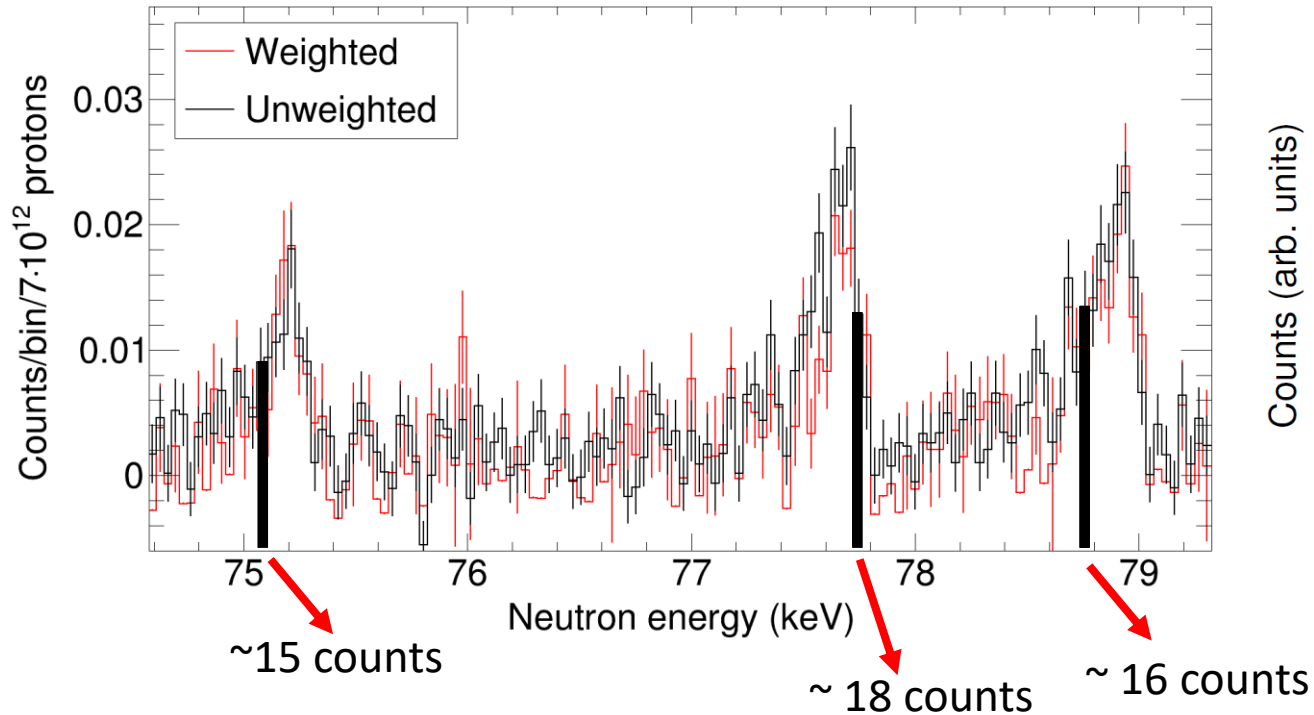


- 100  $\mu\text{m}$  thick  ${}^{197}\text{Au}$  sample  $\rightarrow$  the 4.9 eV resonance **saturates**.
- 80 mm sample to validate the analysis methodology.

$\dagger$ R. L. Macklin, “Absolute neutron capture yield normalization”, Nuclear Instruments and Methods 164(1) (1979)

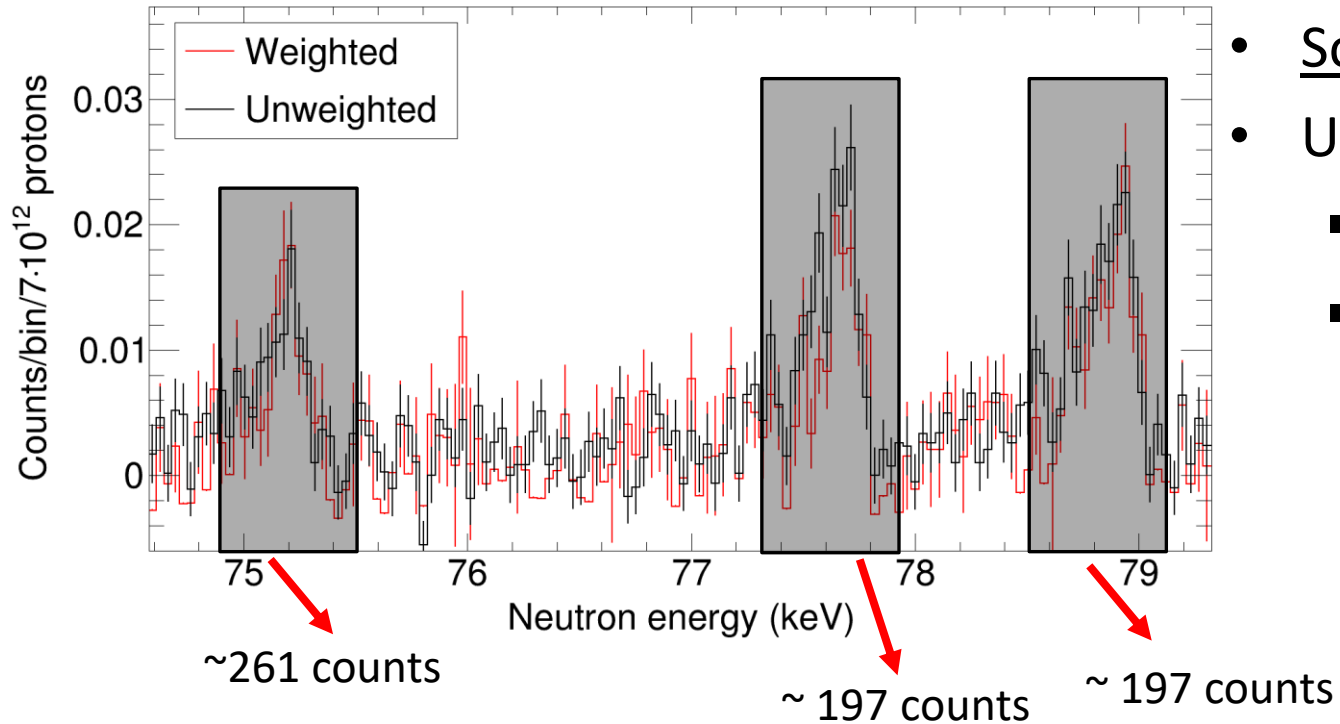
# Backup. Capture yield analysis

The WF enhance the natural statistical fluctuations → Limited statistics bin-by-bin.



# Backup. Capture yield analysis

The WF enhance the natural statistical fluctuations → Limited statistics bin-by-bin.



- Solution: **Average Weighting Factor (AWF)**.
- Used at n\_TOF to extend the energy range.

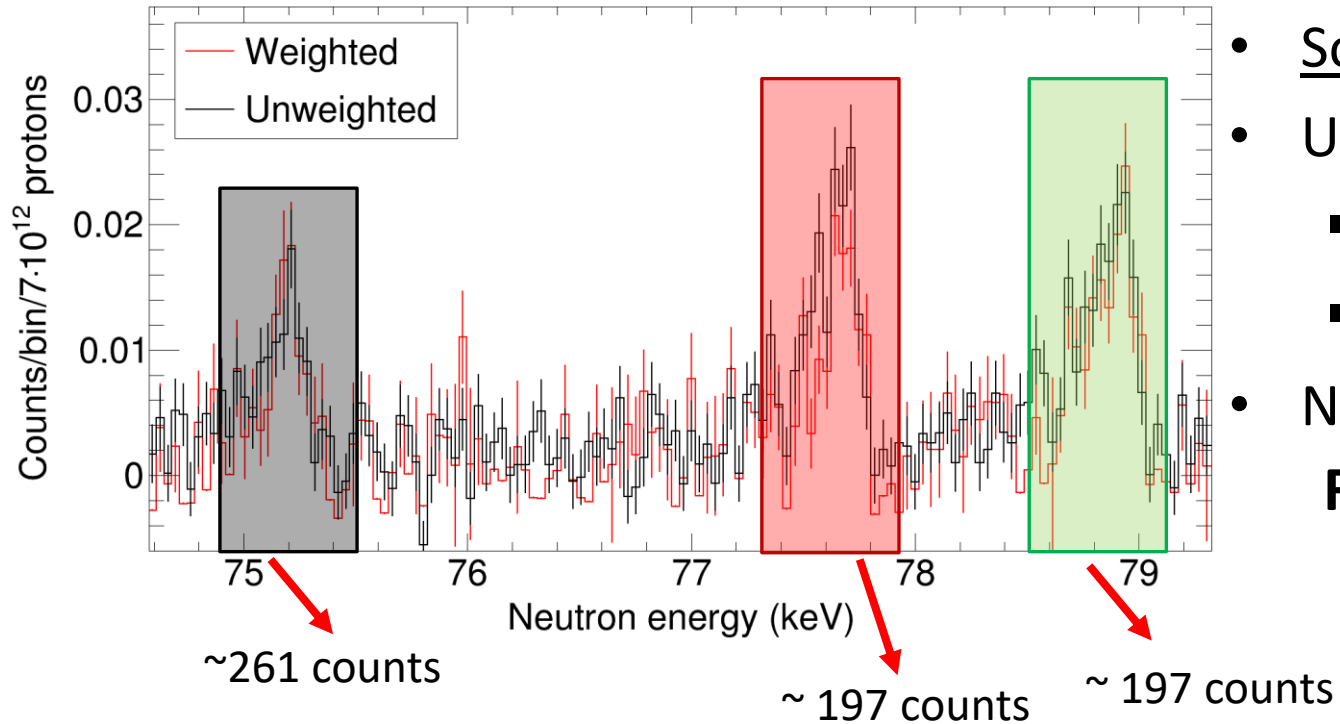
- $J = 0^+$
- Heavy nuclei

Same de-excitation pattern for every resonance

$$WF_{res} = \frac{A_r^{\text{weighted}}}{A_r^{\text{unweighted}}} \rightarrow \langle WF_{res} \rangle$$

# Backup. Capture yield analysis

The WF enhance the natural statistical fluctuations → Limited statistics bin-by-bin.

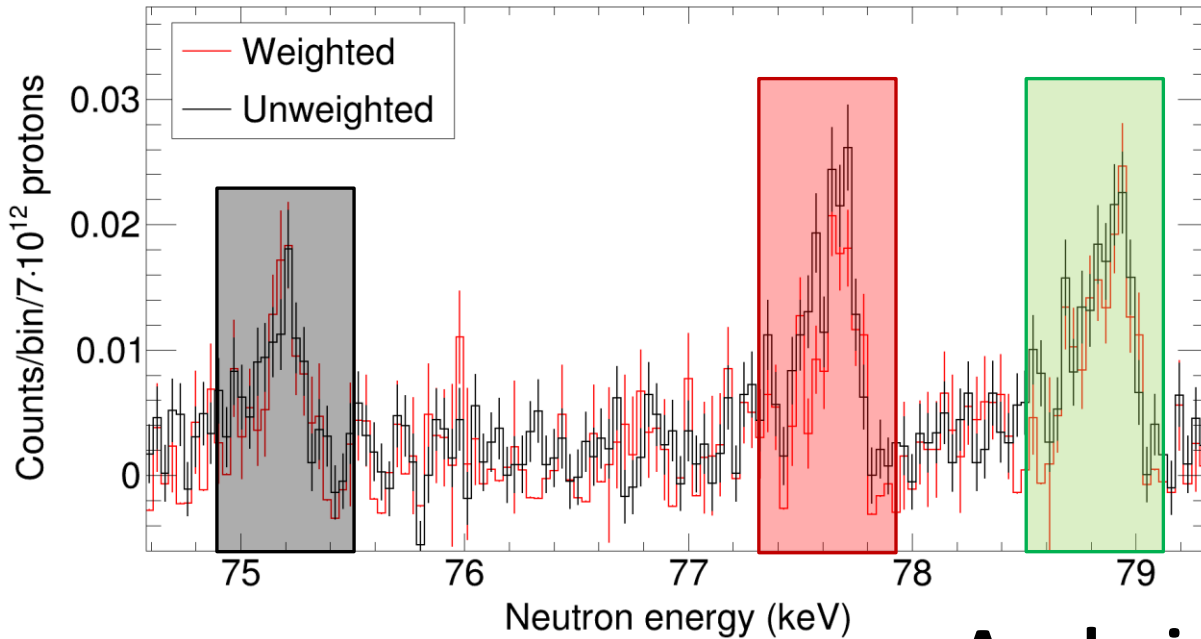


- Solution: **Average Weighting Factor (AWF)**.
  - Used at n\_TOF to extend the energy range.
    - J = 0<sup>+</sup>
    - Heavy nuclei
- Same de-excitation pattern for every resonance
- New technique proposed:  
**Resonance Weighting Factor (RWF)**

$$WF_{res} = \frac{A_r^{\text{weighted}}}{A_r^{\text{unweighted}}} \rightarrow \langle WF_{res} \rangle$$

# Backup. Capture yield analysis

The WF enhance the natural statistical fluctuations → Limited statistics bin-by-bin.



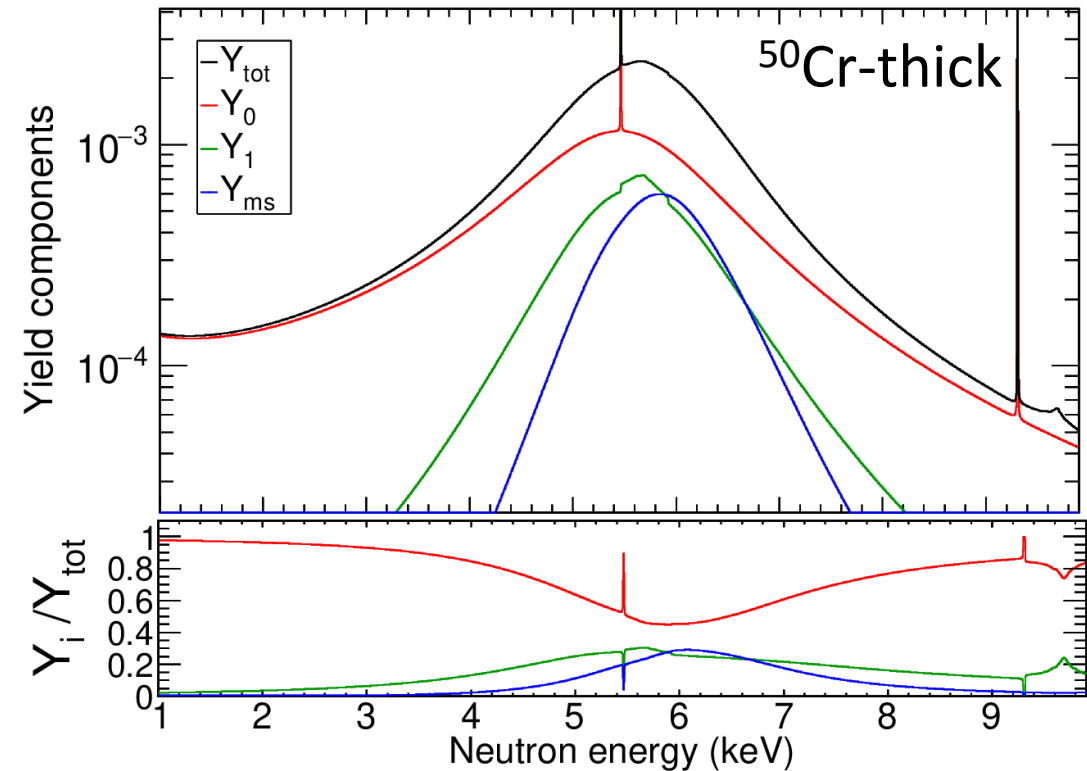
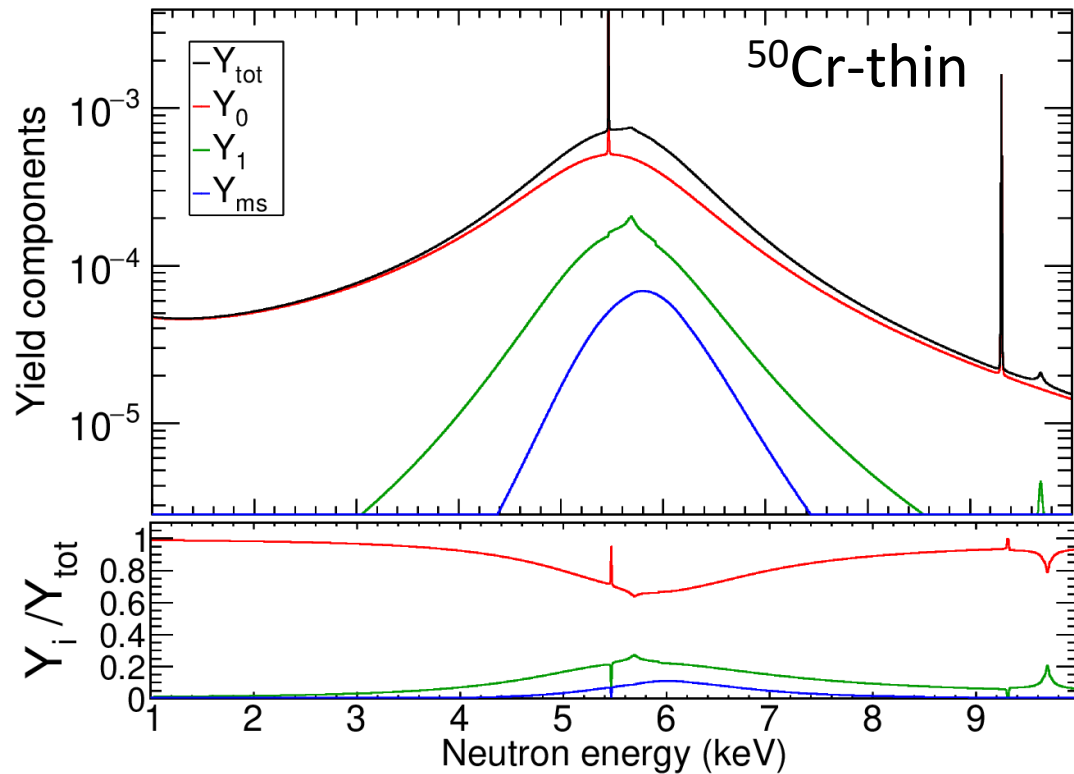
- Solution: **Average Weighting Factor (AWF)**.
  - Used at n\_TOF to extend the energy range.
    - $J = 0^+$
    - Heavy nuclei
- Same de-excitation pattern for every resonance
- New technique proposed:  
**Resonance Weighting Factor (RWF)**

## Analysis strategy

- |                            |        |   |                              |
|----------------------------|--------|---|------------------------------|
| • Very good statistics (6) | → PHWT | } | • Thin samples (1-10 keV)    |
| • Good statistics (42)     | → RWF  |   | • Thick samples (10-100 keV) |
| • Bad statistics (24)      | → AWF  |   | • Thick samples (10-100 keV) |

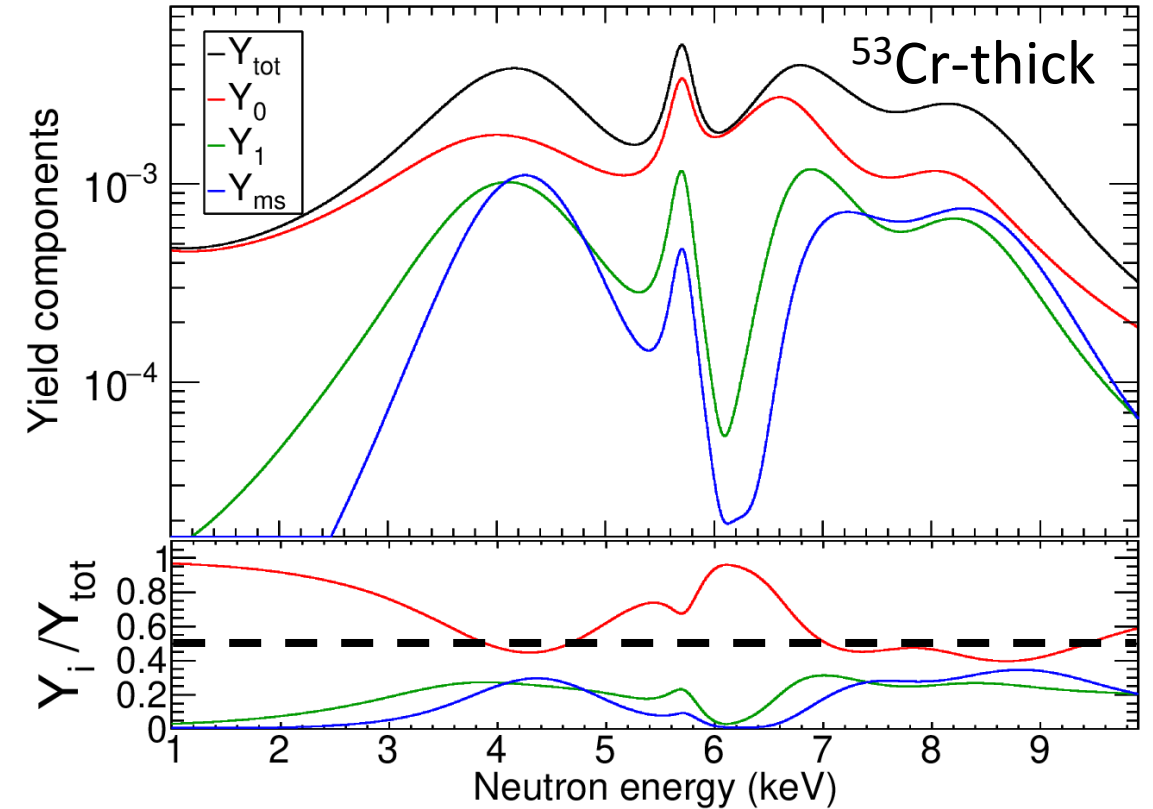
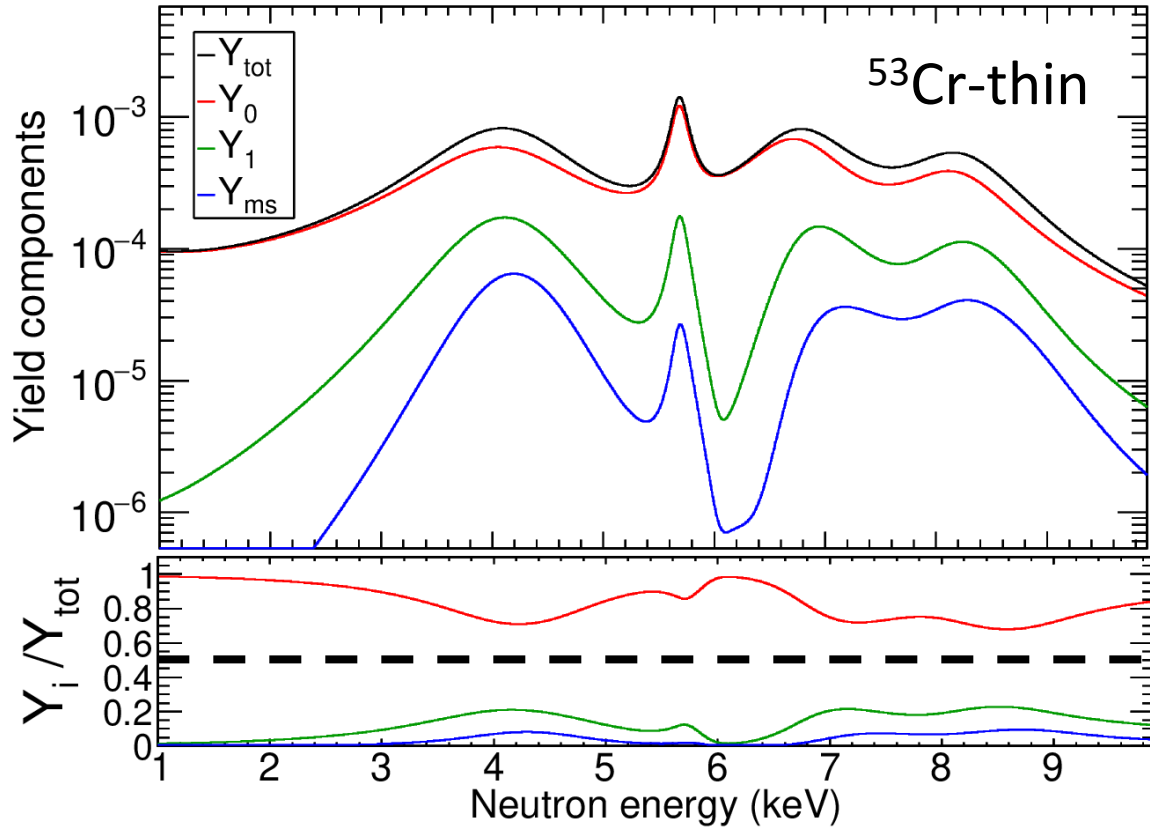
# Backup. Resonance analysis with SAMMY ( $^{50}\text{Cr}$ )

- Main resonance  $\rightarrow$  in agreement with JEFF-3.3 (even  $K_\gamma$  also similar to CENDL-3.2).
- Overestimation by INDEN.
- Previous energy shifted: from  $E_n = 5.621$  keV to  $E_n = 5.581(6)$  keV. } Multiple-scattering effects
- Resonance deformed in the thick sample.



# Backup. Resonance analysis with SAMMY ( $^{53}\text{Cr}$ )

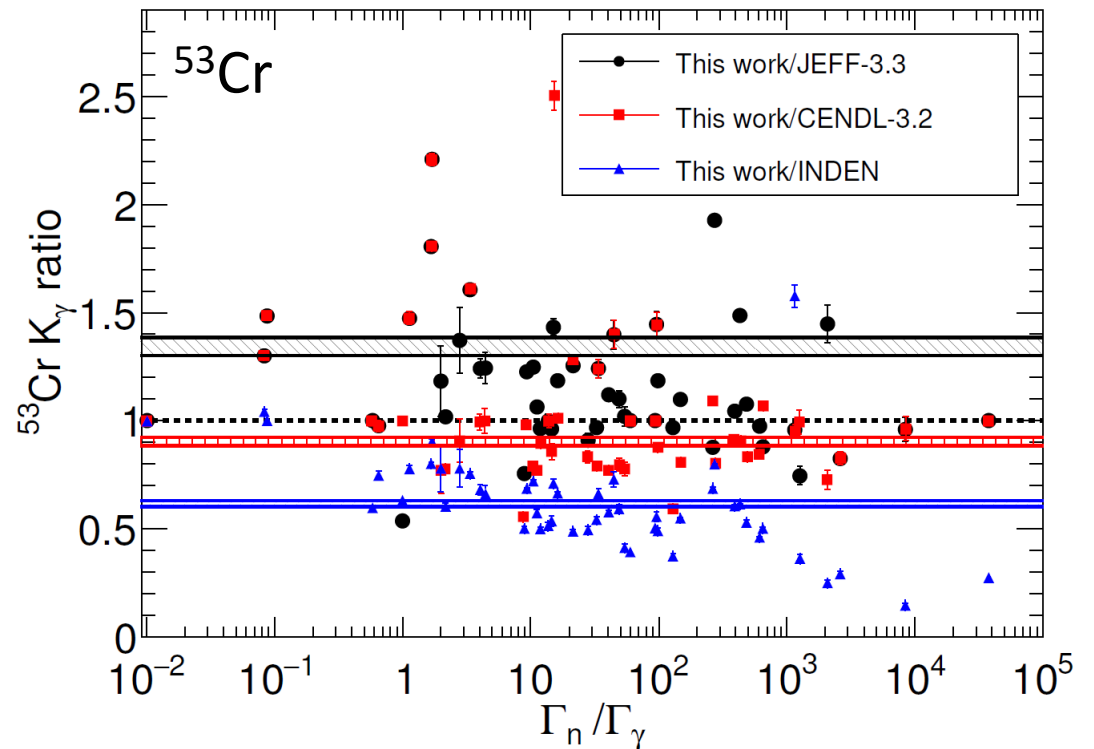
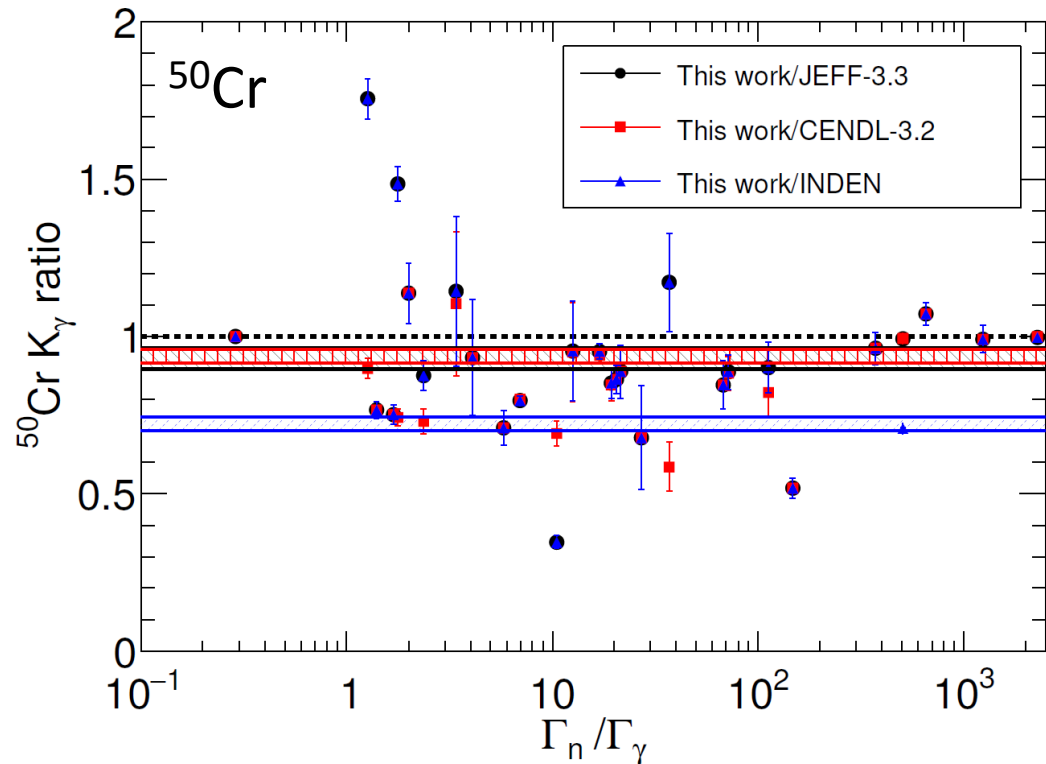
- The MS effects are very large  $\rightarrow$   $\sim 7\text{mm}$  thickness.
- SAMMY fails to accurately evaluate the MS effects.



# Backup. $^{50,53}\text{Cr}(n,\gamma)$ at EAR1 results

$$K_\gamma = g_J \frac{\Gamma_\gamma \Gamma_n}{\Gamma_\gamma + \Gamma_n}$$

- The radiative kernel  $K_\gamma$  gives information resonance by resonance.
- $^{50}\text{Cr} \rightarrow$  7% lower than JEFF-3.3 and CENDL-3.2, 40% lower than INDEN.
- $^{53}\text{Cr} \rightarrow$  35% higher than JEFF-3.3, 10% and 60% lower than CENDL-3.2 and INDEN, respectively.



# Backup. $^{50,53}\text{Cr}$ (n, $\gamma$ ) at EAR1 results

	$^{50}\text{Cr}$ MACS (mb)	$^{53}\text{Cr}$ MACS (mb)
JEFF-3.3 (2017)	38.2	25.9
CENDL-3,2 (2020)	37.7	31.5
INDEN (2023)	45.0	51.7
HiSPANoS(2025)	<b>37.1(20)</b>	-
<b>n_TOF (2025)</b>	<b>35.0(24)</b>	<b>30.9(22)</b>

